# Study on membrane dynamics of vesicles as a soft interface and its application to functional materials

ソフト界面としてのベシクルの膜揺らぎに関する研究と
機能性材料への応用

**Saki Fukuma**

福間　早紀

Graduate School of

Environmental and Life Science, Okayama University

岡山大学環境生命科学研究科

**March 2020**

# Contents

**Chapter 3**

**Evaluation of the effect of polymerization reaction on / in the membrane for vesicle destruction resistance due to vesicle membrane fluctuation**

# Chapter 1
# General introduction

The situation of the world has gradually and absolutely become worse because of the exhaustion of fossil resources, the exhaustion of metal resources for the catalyst, and global warming by the greenhouse gases. Therefore, the measure to the mentioned global problems has been demanded from social to scientific aspects. Specifically, the chemical industry has required the reduction of carbon dioxide efflux, reduction of energy consumption, and reduction of the usage of metal catalysts (or their recycle). The promising options for our world would be the development of the chemical process under the mild condition (room temperature and atmospheric pressure) or exploitation of alternative reaction systems without metal catalysts. There is also a need for chemical processes that reduce the use of organic solvents. Separating the organic solvent after the reaction requires more energy, and even after the separation, the organic solvent is not environmentally friendly, and proper disposal requires additional energy and processes. From the viewpoint of environmental impact, water is the most ideal solvent as the reaction medium. The water is very stable and environmentally friendly. However, there are still some problems with using water as the reaction medium. One problem is that the reaction slows down. The second is that the catalytic ability decreases.

One of the possible developments of the chemical process under the mild conditions is the use of *soft materials* and *soft interfaces*. Soft materials are materials that can be easily deformed by thermal stresses or thermal fluctuations at about room temperature. Soft materials include liquids, polymers, foams, gels, colloids, granular

materials, as well as most soft biological materials, as shown in Figure 1 [Liu *et a*l. 2001, Hamley 2003]. Besides, the interface of soft materias is termed soft interfac*e*. Its remarked property is the dynamic response of structure and/or property of soft materials to the outer stimuli. Recent studies suggests that the soft interfaces have the three-dimensional structure rather than the two-dimensional structure and bulk one [Mitamura *et al*. 2013].



proteins    DNA/RNA    emulsions

Vesicles (liposomes)    Gel (polymer matrix)
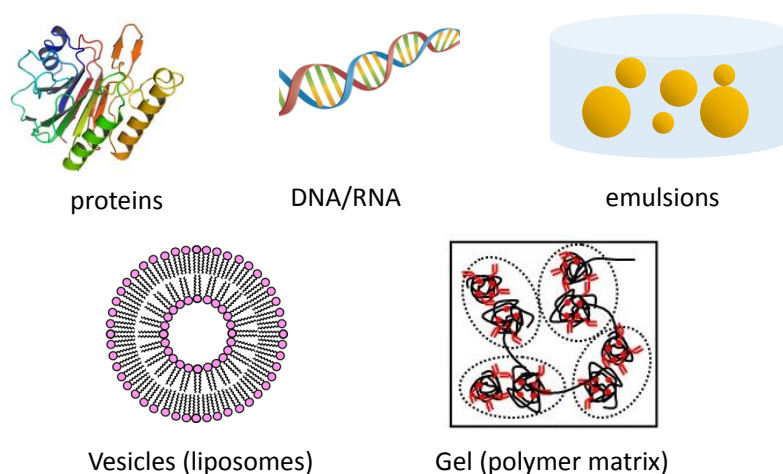
**Figure 1** Typical examples of soft matters / soft interfaces

Three dimensional structure of soft interface affords the interesting phenomena. For examples, the interaction between solvents, ions, or guest molecules, via soft interfaces, dynamically varies the structure and properties of soft materials. Besides, this dynamic change, sometimes acts as the "work". That is, this dynamic change at the soft interfaces can give the driving force of the reaction. In actual, this nature supports the phenomena at the biosystem such as the signal transduction [Groves *et al*. 2010, Eyster 2007], transport of biomolecules [Haan and Slater 2014, Ghale *et al*. 2014], and membrane trafficking [Hanzal-Bayer and Hancock 2007]. These aspects have been

adopted to the development of novel biomaterials [Haris and Chapman 1998] and biodevices [Ghale *et al*. 2014].

However, the research in the molecular aspects has not been fully advanced and given no suggestions to understand the related phenomena. For examples, the significance of the interface has been widely recognized in the field of biomaterials and biosensors. The interfaces at these examples complicatedly relate to the biopolymers, polyelectrolytes, ionic species, water molecules, which makes it difficult to understand the mechanistic details.

Of the phenomena, polymerization reaction at the soft interfaces has been widely studied to understand the above mentioned problems. Polyaniline polymerization is the typical system using soft interfaces such as DNA [Nagarajan *et al*. 2001], micelles [Kim *et al*. 2001], and vesicles [Liu *et al*. 1999, Guo et al. 2009]. Polyaniline can be obtained from the monomeric aniline by the enzymatic and electro-oxidative methods [Guo *et al*. 2009, Jung *et al*. 2003]. Obtained polyaniline includes the conductive polymer and the insulating one. Therefore, the selective production of conductive polymer has been long demanded because the conventional electro-oxidative method favors the insulating polyaniline [Jung *et al*. 2003]. Recently, DNA, micelles or vesicles could selectively produce the target, conductive polyaniline, which is termed the *soft template effect*.

If the soft template effect would be fine-tuning by the structural property of constituent soft materials, vesicles are promising system relative to DNA and micelles. The surface property of DNA can be changes by only the selection of base pair. The property of micelles can be controlled by the diameter, surface charge of surfactants used. The fine tuning of DNA and micelles would be then inevitably limited. In contrast, vesicles can be easily modulated by the lipid composition (lipid species, mixing ratio,

3

diameter, environmental conditions and so on). The mixing of more than two components of lipids induces the two-dimensional phase separation (the formation of microdomain) [Almeida *et al*. 2009] and the deformation of vesicles [Doberiner *et al*. 1993]. Thus, vesicle is a promising system so that its dynamic property can be easily fine tuning.

Vesicle is a closed-lipid bilayer systems. This is a typical system of lipid molecular self-assemblies as shown in Figure 2. Vesicles were pioneered by Bangham in 1964. Vesicles have similar permeability to cations and anions as those found in biological membranes, and have been found to be closed vesicles enclosing an aqueous phase [Bangham *et al*. 1965]. Later, it was found that the permeability of ions changed depending on the lipid composition [Papahadjopoulos *et al*. 1967]. Generally, vesicles are formed by van der Waals force [Walde 2004]. Then, its interface is thermodynamically non-equilibrium system and favors the dynamic flexibility [Shimanouchi *et al*. 2011]. The dynamic interface of vesicles is produced by the lateral diffusion of lipid molecules within a bilayer and the mobility of their headgroup [Stuchly *et al*. 1988, Hianik *et al*. 1997, Shimanouchi *et al*. 2011]. This molecular dynamics within a bilayer forms the crevice / pothole and void, which is a field where the small-sized molecules can pass across the bilayer [Shimanouchi *et al*. 2009, Kupiainen *et al*. 2005] and the protein binds to the bilayer [Shimanouchi *et al*. 2013]. Thus, a hydrophobic environment, such as a lipid membrane surface, provides a reactive site for localizing less polar compounds. It has been suggested that biologically occurring environments can be used as a functional platform to achieve organic synthesis. Furthermore, the nanoscopic environment like crevice / pothole is likey to be useful for the organic reaction [Shimanouchi *et al*. 2019]. The productivity of crevice /

pothole within a bilayer might be related to the soft template effect. However, the mechanistic details has been still unclear.
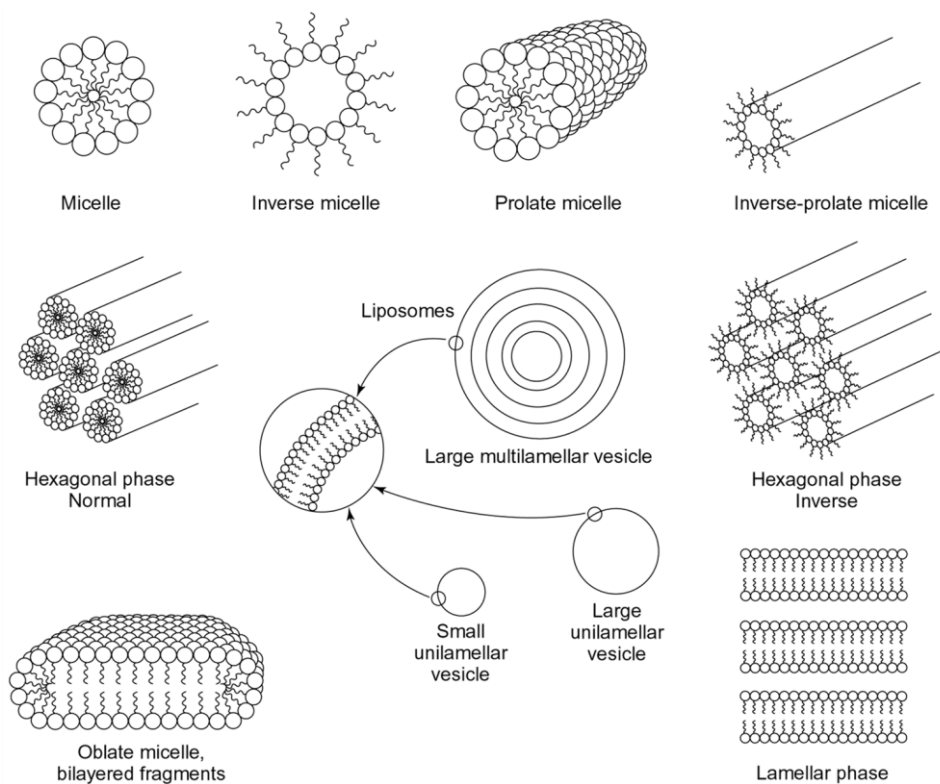


**Figure 2** Typical molecular self-assemblies of surfactants

**Chapter 1    Major objective**
What is a key factor for environmentally benign process using vesicles as a *soft interfaces?*

<Interaction between vesicles with targets>
・Reaction field          ・Separation field          ・Detection field

**Chapter 2**
Effect of membrane dynamics of vesicles on polyaniline polymerization
・*Soft template effect*

**Chapter 3**
Modification of vesicles for stabilization of membrane structure
・*Coverage / Polymerization/ lining structure*

**Chapter 4**
Orientation mechanism of proteins into vesicle membranes
・*electrostatic / non electrostatic manner / undulation*

**Chapter 5**
Relationship between leakage property from vesicles and their undulation
・*sensitivity / selectivity / stability*

**Chapter 6    General conclusion**    Why is vesicles as a *soft interfaces?*

**Figure 3** Frame work of this study

In line with the last sections, the major objective is to clarify the influence of dynamic property of vesicle membranes on the chemical reaction. This is because this objective is useful for developing the environmentally-benign chemical reaction systems. The flow chart of the present study was schematically shown in Figure 3. In Chapter 2, the polyaniline polymerization reaction catalyzed by the horseradish peroxidase was adopted as the case study to understand the soft template effect. According to the biosystem, the production of positively charged polyaniline would interfere the potential difference between inner and outer leaflet of vesicle membranes [Yamashita *et al*. 2002]. It is therefore predicted that the polyaniline polymerization reaction at the vesicle surface induces the instabilization of the vesicle membrane as the reaction field. If so, this drawback should be improved. In Chapter 3, the strategies to

6

reinforce the membrane structure against the chemical reaction at the vesicle surface have been then examined in terms of coverage, polymerization of lipids, and the lining structure of membranes. In Chapter 4, the orientation mechanism of proteins has been studied. The thermodynamic analysis was performed to clarify the (non) electrostatic contribution to the protein-vesicle interaction. Likewise, the contribution of headgroup mobility to the insertion of proteins to vesicle membranes was studied. Finally, the possible mechanism of the interaction between vesicle membranes and protein was submitted based on the crevice / pothole. Here, proteins as case study included the catalyst for enzymatic polymerization reaction of polyaniline. In Chapter 5, the author claried how the protein enhance / suppress the leakage process of entrapped materials. Finally, the author summarized the findings obtained in the present study at Chapter 6. The present findings would be helpful for design and development of novel reaction field, the vehicle for drug delivery, biosensor unit.

# References

Almeida, P. F.; Pokorny, A., Mechanisms of Antimicrobial, Cytolytic, and Cell-Penetrating Peptides: From Kinetics to Thermodynamics. *Biochemistry*, **48**, 8083-8093 (2009)

A.D. Bangham, M.M. Standish and J.C. Watkins, The action of steroids and streptolysin S on the permeability of phospholipid structures to cations. *J. Mol. Biol.*, **13**, 238-252 (1965)

de Haan, H. W.; Slater, G. W., Biomolecule transport across biomembranes in the presence of crowding: Polymer translocation driven by concentration and disorder gradients. *Phys. Rev.*, E **90**, 020601(R) (2014)

Döbereiner, H. G.; Käs, J.; Noppl, D.; Sprenger, I.; Sackmann, E., Budding and fission. *Biophys. J.*, **65**, 1396-1403 (1993)

Eyster, K. M., The membrane and lipids as integral participants in signal transduction: lipid signal transduction for the non-lipid biochemist. *Adv. Physiol. Educ.*, **31**, 5–16 (2007)

Ghale, G.; Lanctôt, A. G.; Kreissl, H. T.; Jacob, M. H.; Weingart, H.; Winterhalter, M.; Nau, W. M., Chemosensing Ensembles for Monitoring Biomembrane Transport in Real Time. *Angew. Chem.*, **53**, 2762-2765 (2014)

Groves, J. T.; Kuriyan, J., Molecular mechanisms in signal transduction at the membrane. *Nature Structural & Molecular Biology*, **17**, 659–665 (2010)

Guo, Z.; R€uegger, H.; Kissner, R.; Ishikawa, T.; Willeke, M.; Walde, P., Vesicles as Soft Templates for the Enzymatic Polymerization of Aniline. *Langumuir*, **25(19)**, 11390–11405 (2009)

Hamley, I. W., Nanotechnology with Soft Materials. *Angew. Chem.*, **42**, 1692-1712

(2003)

Hanzal-Bayer, M. F.; Hancock, J. F., Lipid rafts and membrane traffic. *FEBS Lett*., **581**, 2098-2104 (2007)

Haris, P. I.; Chapman, D., New Biomaterials Based on Mimicry of Biomembrane Components. (*IOS Press, Ohmsha*) 24-32 (1998)

Hianik, T.; Kaatze, U.; Sargent, D. F.; Krivánek, R.; Halstenberg, S.; Pieper, W.; Gaburjaková, J.; Gaburjaková, M.; Pooga, M.; Langel, U., A study of the interaction of some neuropeptides and their analogs with bilayer lipid membranes and liposomes. *Bioelectr. Bioenerg*., **42**, 123-132 (1997)

Jung, H. S.; Shimanouchi, T.; Morita, S.; Kuboi, R., Novel Fabrication of Conductive Polymers Contained Micro‐Array Gas Sensitive Films Using A Micromanipulation Method. *Electroanalysis*, **15**, 1453-1459 (2003)

Kim, B.-J.; Oh, S.-G.; Han, M.-G.; Im, S.-S., Synthesis and characterization of polyaniline nanoparticles in SDS micellar solutions. *Synthetic Metals*, **122**, 297-304 (2001)

Kupiainen, M.; Falck, E.; Ollila, S.; Niemelä, P.; Gurtovenko, A. A.; Hyvönen, M. T.; Patra, M.; Karttunen, M.; Vattulainen, I.; Free Volume Properties of Sphingomyelin, DMPC, DPPC, and PLPC Bilayers. *J. Comp. Theor. Nanosci.*, **2**, 401-413 (2005)

Liu, W.; Cholli, A.L.; Nagarajan, R.; Kumar, J.; Tripathy, S.; Bruno, F. F.; Samuelson, L., The Role of Template in the Enzymatic Synthesis of Conducting Polyaniline. *J. Am. Chem. Soc*. **121**, 11345–11355 (1999)

Liu, Z.; Toh, W.; Ng, T. Y., Advances in Mechanics of Soft Materials: A Review of Large Deformation Behavior of Hydrogels. *International Journal of Applied Mechanics*, **7**, 1530001 (2015)

Mitamura, K.; Yamada, N. L; Sagehashi, H.; Torikai, N.; Arita, H.; Terada, M.; Kobayashi, M.; Sato, S.; Seto, H.; Goko, S.; Furusaka, M.; Oda, T.; Hino, M.; Jinnai, H.; Takahara, A., Novel neutron reflectometer SOFIA at J-PARC/MLF for in-situ soft-interface characterization. *Polymer J.*, **45**, 100-108 (2013)

Nagarajan, R.; Liu, W.; Kumar, J.; Tripathy, S. K.; Bruno, F. F.; Samuelson, L. A., Manipulating DNA Conformation Using Intertwined Conducting Polymer Chains. *Macromolecules*, **34**, 3921-3927 (2001)

D. Papahadjopoulos and J.C. Watkins, Phospholipid model membranes. II. Permeability properties of hydrated liquid crystals. *Biochem. Biophys. Acta*, **135**, 639-652 (1967)

Shimanouchi, T.; Ishii, H.; Yoshimoto, N.; Umakoshi, H.; Kuboi, R., Calcein permeation across phosphatidylcholine bilayer membrane: Effects of membrane fluidity, liposome size, and immobilization. *Coll. Surf. B*, **73**, 156-160 (2009)

Shimanouchi, T.; Sasaki, M.; Hiroiwa, A.; Yoshimoto, N.; Miyagawa, K.; Umakoshi, H.; Kuboi, R., Relationship between the mobility of phosphocholine headgroups of liposomes and the hydrophobicity at the membrane interface: A characterization with spectrophotometric measurements. *Coll. Surf. B*, **88**, 221-230 (2011)

Shimanouchi, T.; Umakoshi, H.; Kuboi, R., Growth Behavior of Giant Vesicles with Electroformation Method: Effect of Proteins on Swelling and Deformation. *J. Coll. Int'f Sci.*, **394**, 269-276 (2013)

Shimanouchi, T.; Kitagawa, Y.; Kimura, Y., Application of liposome membrane as the reaction field: A case study using the Horner–Wadsworth–Emmons reaction. *Jounal of Bioscience and Bioengineering*, **128**, 198-202 (2019)

Walde, P.; Umakoshi, H.; Stano P.; Mavelli, F., Emergent properties arising from the assembly of amphiphiles. Artificial vesicle membranes as reaction promoters and

regulators. *Chem.Commun.,* **50,** 10177-10197 (2014)

Yamashita, Y.; Masum, S. M.; Tanaka, T.; Yamazaki, M., Shape Changes of Giant Unilamellar Vesicles of Phosphatidylcholine Induced by a De Novo Designed Peptide Interacting with Their Membrane Interface. *Langmuir*, **18**, 9638-9641 (2002)

# Chapter2

# Effect of dynamic interface of vesicle on
# polyaniline polymerization reaction

## 1. Introduction

For a sustainable society, more environmentally friendly catalysts and materials used in the development and chemical industries are required. For this reason, the shift to highly functional catalysts with soft interfaces has been attracting attention, as opposed to the currently used metal catalysts with rigid hard interfaces. The soft interface has been studied as a material that has a soft interface of gas / liquid, liquid / liquid, etc., and has the characteristic of having a dynamic structure such as phase separation [Himeno *et al.* 2014, Yanagisawa *et al.* 2007]. It is expected to exhibit new functions different from the conventional hard interface. In recent years, it has been required to establish a new interface design guideline for achieving molecular recognition and highly selective separation by utilizing these characteristics, and it is expected that the method will be applied to artificial organs and biosensors as an application method [Otero *et al.* 2012]. One of the notable functions of the soft interface is the control of the reaction selectivity by the interface composition, which has been reported as a soft template effect of the soft interface [Guo *et al.* 2009].

In this study, we focused on the polymerization reaction of polyaniline as an example using the soft template effect of the soft interface. Among the conductive polymers, polyaniline has attracted attention because it is water-soluble and its properties can be controlled by its oxidation state [Anagmostopoulos *et al.* 1998]. Polyaniline can be synthesized chemically or electrochemically under strong acid

conditions [Zotti *et al.* 1988]. However, in recent years, methods using enzymes obtained from plants have attracted attention [Jin *et al.* 2001]. Enzymes are characterized by their ability to provide environmentally friendly room temperature reaction conditions, advanced reaction rate control, and higher product yields, and have been studied for use as biological catalysts in the synthesis of polyaniline [Jin *et al.*, 2001]. Horseradish peroxidase (HRP) can catalyze the oxidation of a wide range of compounds including aromatic amines and phenols in the presence of hydrogen peroxide [Mita *et al.* 2002]. In this study, we decided to carry out enzymatic polymerization using HRP based on the existing literature [Guo *et al.* 2009].

Vesicles have a soft interface and are one of the eco-friendly co-catalysts and materials [Kaneda *et al.*, 2000, Walde *et al.* 2014, Erb *et al.*, 2000, Olea *et al.* 2008]. Vesicles are composed of lipid bilayer membranes. It has been shown that the soft interface of vesicles has various soft template effects that are useful for chemical processes using its dynamic structure [Guo *et al.*, 2009]. This differs from the mold effect of the hard interface, for example, by changing the composition of the vesicles to increase the selectivity of products and reduce the production of by-products [Guo *et al.*, 2009]. However, it is a problem that the condition of the soft template effect is unclear, and it is expected that clarification of the expression condition will provide a design guide for functional materials with soft interfaces.

In the polyaniline enzymatic polymerization reaction using vesicles, not only the partially oxidized conductive emeraldine salt but also the insulating pernigraniline salt was polymerized. Systems that selectively polymerize emeraldine salt using the soft template effect of the soft interface have been studied [Guo *et al.*, 2009]. According to the group of Liu *et al.*[1999], It is said that "micelles and vesicles provide

a local environment where the surrounding pH and charge are different from those of the bulk," and this is used as the vesicle soft template effect. However, the mechanism by which the selectivity of the polymerization reaction changes has not been elucidated.

It has been reported that the dynamics of the vesicle membrane interface controls the three-dimensional structure and reactivity of the enzyme [Shimanouchi *et al*. 2010] and amyloid formation [Shimanouchi *et al*. 2012]. On the other hand, it has been reported that enzymes and proteins induce morphological changes in vesicles [Holopainen *et al*. 2000, Shimanouchi *et al*. 2013]. Thus, there seems to be a correlation between the reaction on the vesicle membrane and the interface dynamics of the membrane. The dynamics of the membrane are (i) microscopically, the flow state generated by lipid molecules [Helfrich *et al*. 1973], and (ii) macroscopically, the membrane fluctuations generated by the entire membrane structure [Helfrich *et al*., 1973, Faucon *et al*. 1989]. Giant vesicles (GVs; particle size 1 μm or more) can visualize macroscopic membrane fluctuations, and may reveal some of the mechanisms of the template effect.

In this chapter, I studied the effect of dynamic interface of vesicle on polyaniline polymerization reaction. In order to verify the relationship between the vesicle membrane fluctuation and the reaction process, we performed a kinetic analysis of the polymerization reaction and a vesicle membrane fluctuation analysis using GVs that can be observed with a microscope. Next, the interaction between the enzyme (protein) and the membrane was examined, and the soft template effect of the soft interface in the enzymatic polymerization reaction was evaluated.

## 2. Materials and Methods

### 2.1 Materials

The lipids and reagents used were 1,2-dioleoyl-*sn*-glycero-3-phosphocholine (DOPC), 2-oleoyl-1-palmitoyl- *sn*-glycero-3-phosphocholine (POPC), sorbitan monolaurate(Span20), polyoxyethylene sorbitan monolaurate (Tween20), sorbitan monopalmitate (Span40), polyoxyethylene sorbitan monopalmitate (Tween40), sorbitan monooleate (Span80), polyoxyethylene sorbitan monostearate (Tween60), decanoic acid (DA), 1,2-dioleoyl-3-trimethylammonium-propane (chloride salt) (DOTAP) and peroxidase from horseradish (HRP) were purchased from Wako Pure Chemicals Ltd (Osaka, Japan). 1,2-Dipalmitoyl-sn-glycero-3-phosphocholine (DPPC), 1,2-dimirystoyl-sn-glycero-3-phosphocholine (DMPC), 2-dioleoyl-sn-glycero-3-[phosphor-rac-(3-lysyl(1-glycerol))] (DOPG), sodium dodecylbenzene sulfonate (SDBS), sodium di-2-ethylhexylsulfosuccinate (AOT) were purchased from Tokyo Chemical Industry Co., Ltd. (Tokyo, Japan). Phosphorylcholine self-assembled monolayers (PC-SAM), poly(2-methacryloyloxyethyl phosphorylcholine) 10mer: *n*= 10) (PMPC10), PMPC50 and PMPC100 were provided by Professor Madoka Takai (University of Tokyo).

### 2.2 Giant vesicle (GVs) Preparation

The lipid was dissolved in chloroform, and the lipid membrane was placed in a round-bottom flask using an evaporator. After allowing to stand overnight, giant vesicles (GVs) were prepared by allowing them to stand in a constant temperature bath at 70 °C. for 4 hours by the high-temperature hydration method [Hub *et al.* 1982]. A dispersion with an average particle size of about 10 µm and a concentration of 10 mM

15

was prepared.

## 2.3 Lipid planar membrane formation

A glass substrate (Matsunami Glass Co., Ltd.) was immersed in a 1-decanethiol / ethanol solution (2 mM) to form a thiol self-assembled film. A thiol self-assembled monolayer is a type of self-assembled monolayer (SAM), which is a self-assembled monolayer that is formed spontaneously when a substrate is immersed in a solution. In addition, it is thought that this membrane can easily obtain a highly oriented monomolecular film and show high stability, so that it is easy to form a lipid membrane with high alignment on the substrate. Next, the substrate was immersed in a lipid / chloroform solution (10 mM), dried, washed with water, and dried to form a planar lipid membrane.

## 2.4 Vesicle Preparation

A solution of lipids in chloroform was dried in a round-bottom flask by rotary evaporation under vacuum. The obtained lipid thin film was kept under high vacuum for at least 12 h , and then hydrated with distilled water at room temperature. The obtained liposome suspension was frozen at -80℃ and then thawed at 45℃～60℃ ; this freeze-thaw cycle was repeated 5 times. A large unilamellar vesicle was obtained by extruding the vesicle suspension 15 times through 2 layers of a polycarbonate membrane with a mean pore diameter of 100 nm using an extruding device (LiposoFast-Basic; ADVAMTEC)

## 2.5 Polyaniline polymerization

Reaction conditions were as previously described [Guo *et al*., 2009]. GVs (10 mM), aniline (40 mM), aqueous solution of sodium dihydrogen phosphate ($NaH_2PO_4$ 0.1 M), horseradish peroxidase (HRP) (5 mg / ml), and hydrogen peroxide (0.2 M) were stirred at room temperature for 5 h. Final concentrations were GVs ($2.285 \times 10^{-3}$ mol / L), aniline ($2.285 \times 10^{-3}$ mol / L), HRP (0.04286 mg / mL), and $H_2O_2$ (1.714 mmol / L).

## 2.6 UV-vis measurement

The absorbance of the obtained polyaniline solution was measured at multiple wavelengths by UV-VIS (U-2000A manufactured by Ultraviolet visible Absorption Spectroscopy HITACHI). According to the previous report [Guo *et al*., 2009], three points of 520 nm (pernigraniline salt) and 1000 nm (emeraldine salt) were selected. The measurement was performed every minute from 0 minutes to 10 minutes, and the reaction rate constant was determined.

## 2.7 Microscopic observation

GVs size and morphological changes upon protein addition were observed using an inverted research microscope system IX73 Olympus Corporation (including digital camera D.P80-SET-A / MVDOC software). The reaction was performed under the same concentration conditions as in the polyaniline polymerization experiment as described in Sec. 2.5.

## 2.8 Measurement of membrane elastic modulus by membrane fluctuation analysis

The fluctuation of the film was discussed by measuring the film elastic coefficient $k_c$ according to the previous method [Faucon *et al*. 1989]. Briefly, using the radius $\rho(\varphi, t)$ of the vesicle at a certain time $t$ and the radius $\rho(\varphi + \gamma, t)$ at a position shifted by an angle therefrom, the correlation function $\xi(\gamma, t)$ can be defined as described in Sec. 3.5.2. Using the time average $\xi(\gamma)$ of $\xi(\gamma, t)$, the membrane elastic coefficient $k_c$ can be obtained from **equation (2-2)**.

$$\xi(\gamma, t) = \frac{1}{R^2}\left[\int_0^{2\pi} \rho(\varphi + \gamma, t)\rho(\varphi, t)d\varphi - \rho^2(t)\right] \quad \textbf{(2-1)}$$

$$\xi(\gamma) = <\xi(\gamma, t)> = \frac{kT}{4\pi k_c}\sum_{n=2}^{n_{max}} f(n, \sigma)P_n(cos\gamma) - (Correction\ term) \quad \textbf{(2-2)}$$

$R$ is the vesicle radius. $f(n, \sigma)$ is a function of natural number $n$ and membrane tension $\sigma$, and $P_n(x)$ is a Legendre polynomial. The effect of the focus of the objective lens deviating from the true center of the vesicle was corrected by the correction term in **equation (2-2)**.

## 2.9 Surface pressure analysis

Surface pressure analysis was performed to determine the $\pi$-A isotherm, and protein orientation analysis was performed by Small LB film making device FSD-220C (U.S.I Corp.) and LB LIFT CONTROLLER FSD-23(U.S.I Corp.) according to the previous report [Phillips and Chap Man 1968]. First, 60 μL of lipid (1 mM) dissolved in chloroform was dispersed in a water tank filled with ultrapure water. After allowing the lipid to stand at the gas-liquid interface for 15 minutes, pressure was applied to the surface with a barrier to investigate the change in occupied area (*A*) due to the change in the surface pressure ($\pi$). Lipid was dispersed and allowed to stand for 15 min, then 60 μL of protein solution (HRP: 5 mg / mL) was added to the water bath,

after 5 min left, Similarly, changes in $A$ due to changes in $\pi$ were investigated, and the orientation pattern of proteins was discussed from the curve change due to the presence or absence of protein.

## 2.10 Polymerization measurement using MALDI - TOFMS

Molecular weight of polyaniline was investigated by using MALDI-TOF MS (Autoflex II, Bruker Daltonics Co. Ltd.). To stop the polymerization reaction after 30 min, 10-15 wt % aqueous $NH_4OH$ containing 1 wt% LiCl (0.5 mM) was added to the reaction mixture (3mL) to deprotonate polyaniline. The precipititate was collected by centrifugation (300 rpm), followed by vacuum drying.

## 2.11 Zeta Potential measurement

Using the lipids of entries 3, 7, 12, and 15, 100-nm liposomes (10 mM) were prepared by the method described in Sec. 2.4. The zeta potential of the vesicles was measured using Zetasizer Nano (ZEN3600; MALVERN).

## 3. Results and Discussion

### 3.1 GVs soft template effect

First, enzymatic polymerization of polyaniline was performed using GVs under the same conditions as those using 100-nm vesicles based on previous literature [Guo *et al*. 2009]. In previous literature, emeraldine salt was formed when SDBS or SDS was used [Guo *et al*. 2009]. Similar results were obtained in this study. Therefore, it is suggested that GVs show the same template effect as 100 nm vesicles. **Table 2-1** shows the products obtained under various conditions (no GV or various GV). As a result, insulators pernigraniline salts (PS) were formed in $NaH_2PO_4$ (no-GVs), NaH2PO4/1, 4-dioxane(1:1) (no-GVs), POPC-GVs, DOPC-GVs, DOPG-GVs, Span20/Tween20 (75:25)-GVs, Span40/Tween40 (75:25)-GVs and Span80/Tween60 (75:25)-GVs, while emeraldine salts (ES) were formed in SDBS/DA (1:1)-GVs, SDBS/DA (75:25)-GVs and AOT-GVs (**Figures 2-1, 2-2**). These results indicate that mixing vesicles alone cannot control the reactivity of ES suggesting that the type of lipid used in vesicles must be examined.

When SDBS / decanoic acid-GVs and AOT-GVs were co-present, they quickly changed to a green suspension peculiar to ES. These GVs have a negative charge, and a black-purple PS was also observed in DOPG-GVs, which also had a negative charge. Therefore, it was shown that ES cannot be formed selectively only under the condition with negative charge. In addition, in order to confirm the possibility that the difference in membrane structure may affect the reactivity, we examined GVs composed of phospholipids (DOPC-GVs, POPC-GVs and DOPG-GVs) and GVs composed of surfactants (Span20/Tween20 (75:25)-GVs, Span40/Tween40 (75:25)-GVs and Span80/Tween60 (75:25)-GVs). In each case, PS was formed. From

these results, it was shown that ES could not be advantageously produced only by using a surfactant.
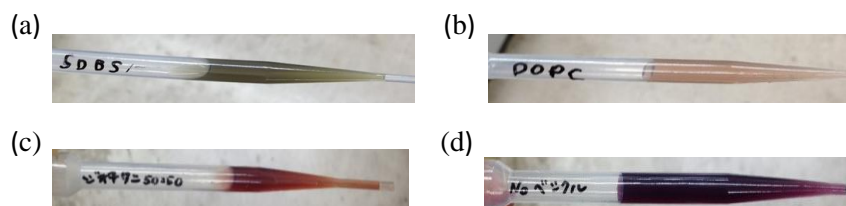
(a)

(b)

(c)

(d)



**Figure 2-1 Soft template effect of GVs on polyaniline polymerization** (a) Solution using SDBS / decanoic acid(1:1)-GVs (green) (b) Solution of control system (no vesicle, sodium dihydrogen phosphate: dioxane (1: 1) (black purple) (C) Solution with DOPC-GVs (black purple) (d) Solution of control system (no vesicles) (black purple)

## 3.2 Kinetic analysis of polyaniline polymerization using vesicles

In order to quantitatively compare the reaction rates of the products under each polymerization reaction condition, the wavelength during the polymerization reaction was measured using a spectrophotometer (Ultraviolet visible Absorption Spectroscopy HITACHI, U-2000A). Since ES has a specific absorbance at 1000 nm and PS has a specific absorbance at 520 nm, the formation behavior can be discussed kinetically by tracking the absorbance [Guo *et al.*, 2009]. In this study, for simplicity of discussion, we assumed that the process of formation of ES and PS was first-order kinetics. **Table 2-1** shows the obtained reaction rate coefficients. As a result, a remarkable increase in the rate of ES formation was observed when SDBS/DA (1:1)-GVs, SDBS/DA (75:25)-GVs and AOT-GVs were used, as compared with the case where no vesicles were used. Such an increase in the rate coefficient was not observed in DOPC-GVs, POPC-GVs, DOPG-GVs, Span20/Tween20 (75:25)-GVs, Span40 / Tween40 (75:25) - GVs and Span80/Tween60 (75:25)-GVs were used. From

these experimental results, it was shown by quantitative comparison that there was a soft-template effect such as selective polymerization of ES when SDBS/DA (1:1)-GVs, SDBS/DA (75:25)-GVs and AOT-GVs were used (**Figure 2-2 (a)**).

The reaction rate coefficient ($k_{1000}$) of emeraldine salt formation divided by the reaction rate coefficient of PS ($k_{520}$) was determined as the selectivity of ES formation for each polymerization reaction condition (**Table 2-1**). Then, when DOPC-GVs, POPC-GVs, DOPG-GVs, Span20/Tween20 (75:25)-GVs, Span40 / Tween40 (75:25) - GVs and Span80/Tween60 (75:25)-GVs were used, the selectivity of ES formation ($k_{1000}/k_{520}$) was lower than when GVs was not used, when SDBS/DA( 1:1)-GVs, SDBS/DA (75:25)-GVs and AOT-GVs were used, the reaction selectivity of ES was increased (**Figure 2-2 (b)**).
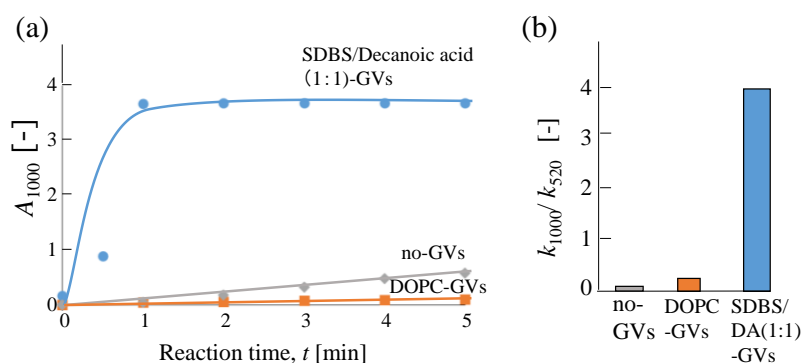


**Figure 2-2 Kinetic analysis of polyaniline polymerization using vesicles**

(a) Comparison of emeraldine salt production (b) Comparison of emeraldine salt selectivity

**Table 2-1 Product and reaction rate coefficient**

| entry | Lipid composition of GVs | Products | $k$ [s$^{-1}$] | |
| --- | --- | --- | --- | --- |
| | | | 1000 nm | 520 nm |
| 1 | NaH$_2$PO$_4$(no-GVs) | PS | 0.43 | 8.13 |
| 2 | NaH$_2$PO$_4$/1,4-dioxane (1:1) (no-GVs) | PS | 0.43 | 0.33 |
| 3 | POPC | PS | 0.31 | 7.49 |
| 4 | DOPC | PS | 0.61 | 3.00 |
| 5 | DOPG | PS | 1.44 | 6.19 |
| 6 | Span20/Tween20 (75:25) | PS | 0.63 | 3.30 |
| 7 | Span40/Tween40 (75:25) | PS | 0.50 | 7.22 |
| 8 | Span80/Tween60 (75:25) | PS | 0.70 | 15.9 |
| 9 | SDBS/DA (1:1) | ES | 1.37 | 0.34 |
| 10 | SDBS/DA (75:25) | ES | 1.30 | 0.90 |
| 11 | AOT | ES | 0.53 | 2.13 |
| 12 | DOTAP | | | |

PS: Pernigraniline salt, ES: Emeraldine salt

## 3.3 Effect of hydrophobic environment on selectivity of polyaniline enzymatic polymerization

To determine whether only the hydrophobic environment of the vesicle membrane affected the increase in the selectivity of ES, the dielectric constant of the solvent was 1: 1 of the aqueous solution of sodium dihydrogen phosphate to dioxane. As a result of experiments, the PS was formed even when polymerization was performed in such a low dielectric constant environment. These results indicated that

polymerization of ES was not possible simply by reacting in a hydrophobic environment, and that the hydrophobic environment in the vesicle membrane was not the only factor required.

**3.4 Effect of the membrane undulation on polyaniline enzymatic polymerization**

The morphological change of GVs relating to the production of ES originates from the amplified undulation of lipid membranes [Shimanouchi *et al*. 2013]. Therefore, we tested the impact of the planar membrane on the selectivity of ES to PS because the planar membrane indicates no undulation. **Table 2-2** shows a comparison of selectivity of ES to PS between vesicle- and planar membrane systems. Overall, black purple-colored suspensions were observed in all systems, indicating the production of PS even in the case of vesicles that indicated the selectivity of ES. Therefore, these results suggested that the undulation of vesicle membranes played an important role for the production of ES.

The author also tested the impact of the lateral diffusion of phospholipid and DA molecules by using the PC- and carboxythiol-SAMs, respectively. The resulting selectivity yielded PS as the main product, as shown in **Table 2-2**. By comparing with phospholipid- and surfactant-planar membranes bearing the fully lateral diffusion, the lateral diffusion appeared to give no impact to the production of ES.

From these results, the membrane undulation enough to induce the morphological change was likely to be a key factor for the improved selectivity of ES to PS.

**Table 2-2 A comparison of selectivity of ES/PS between GVs and planar membranes**

| Lipid composition | Production* | |
|---|---|---|
| | GVs | Planar membranes |
| DOPC | PS | PS |
| SDBS/DA (1:1) | ES | PS |
| AOT | ES | PS |
| PC-SAM | PS | PS |
| PMPC-10 | PS | PS |
| PMPC-100 | PS | PS |
| PMPC-1000 | PS | PS |

PS: Pernigraniline salt, ES: Emeraldine salt

## 3.5 Dynamics of GVs induced by polymerization reaction of aniline

### 3.5.1 Effect of polyaniline polymerization reaction on morphology of GVs

The chemical reaction on the vesicle membrane of oleic acid/oliate-GVs gives an impact on the morphological change of GVs [Peterlin *et al*. 2009]. The same is true for the polymerization of proteins [Cortese *et al*. 1989]. The morphological change of GVs over the polyaniline polymerization is then expected. A direct observation of GVs was then conducted to confirm the morphological change of GVs in the polyaniline polymerization reaction.

First, the addition of $H_2O_2$ induced no morphological change of GVs (data not shown). The addition of HRP to GVs also induced no definite deformation (data not shown). The significant undulation of membranes of GVs after addition of both HRP

and $H_2O_2$ was observed for SDBS/DA-GVs (see the inserted photographs in **Figure 2-3 (b)**). The successive budding of daughter vesicles from parent vesicle was observed. As shown in **Figure 2-4**, the budding from parent vesicle resulted in its volumetric reduction (**points 2-4**). Other GVs prepared by surfactant (entries 10 and 11) indicated not the budding / fission of vesicle membranes but their amplified undulation.

In contrast, DOPC-GVs induced no significant morphological change (**Figure 2-3 (a)**). A small reduction of volume of GVs by at most 20% was observed (**Figure 2-4**). This volumetric reduction was considered to derive from the osmotic effect by additives.

Thus, these observations suggested that the production of ES related to the morphological change of GVs.
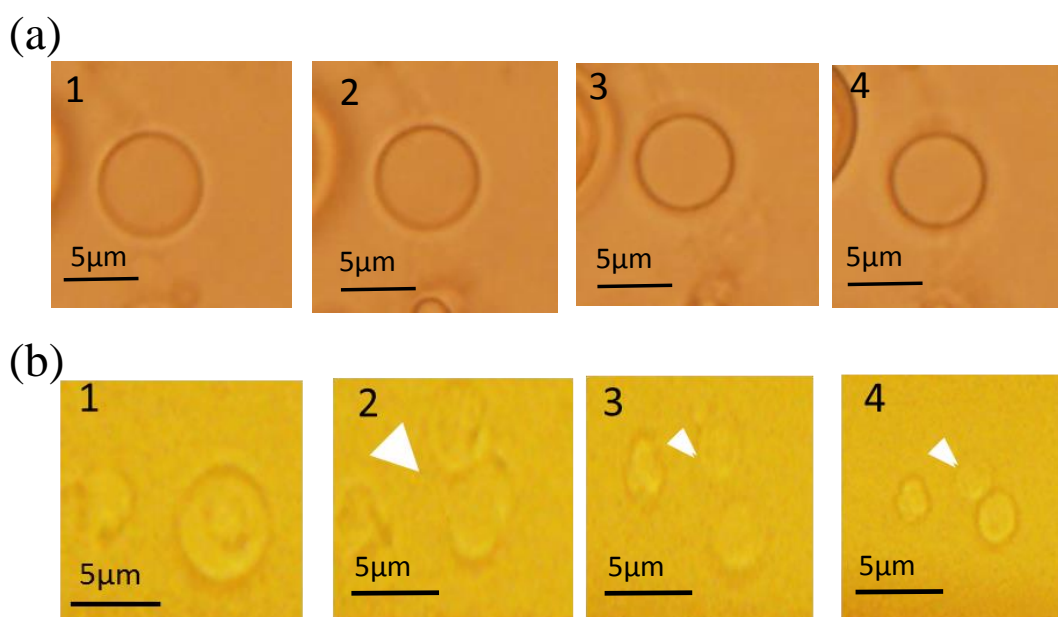


**Figure 2-3 Time-laps images of deformation of GVs over the polyaniline enzymatic polymerization.** (a) DOPC-GVs (b) SDBS/Decanoic acid-GVs
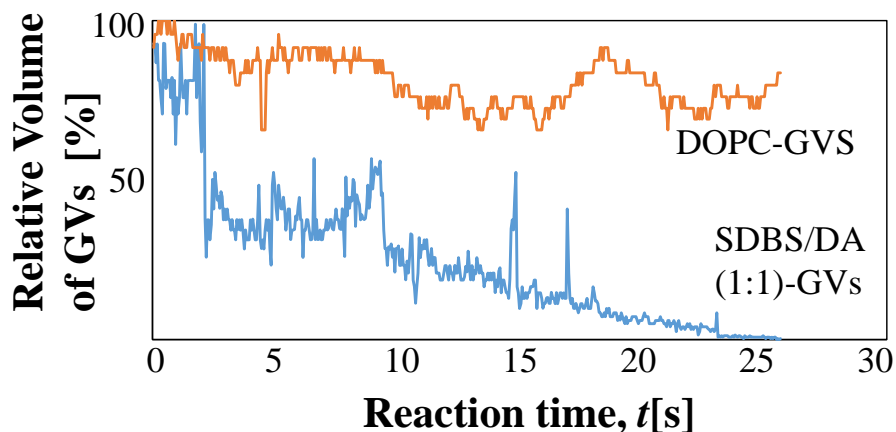
**Figure 2-4 Volumetric change of GVs over polyaniline polymerization reaction**

**(DOPC-GVs: entry 4; SDBS/DA-GVs(1:1): 9).**

### 3.5.2 Effect of HRP addition on membrane elasticity of GVs

The membrane undulation depends on the membrane elasticity [Faucon *et al*. 1989]. The membrane elasticity can be quantified as the $k_c$ value, according to **equations (2-1) and (2-2)** [Faucon *et al*. 1989]. In this section, the membrane elasticity of GVs with and without HRP was evaluated by the $k_c$ value.

By using the microscopic images (**Figure 2-5 (a)**), the mean $k_c$ value of at least 200 vesicles was assessed according to the deviation of the contour of GVs to the true circle (**Figure 2-5 (b)**). The mean value of $k_c$ obtained for SDBS/DA- and DOPC-GVs was $2.40 \times 10^{-18}$ and $1.54 \times 10^{-18}$ J, respectively (**Figures 2-5 (c), Table 2-3**). The result concerning DOPC-GVs is roughly consistent with the previous report [Heeger *et al*. 2001]. The SDBS/DA-GVs had almost the same $k_c$ value as DOPC-GVs. Meanwhile, the addition of HRP externally to SDBS/DA-GVs obviously reduced the $k_c$ value (**Figure 2-3 (b), Table 2-3**). In contrast, DOPC-GVs had no significant reduction of $k_c$

value (**Figure 2-3 (a), Table 2-3**). Generally, GVs with small $k_c$ value easily show the morphological change by the amplifie undulation of membranes [Karami *et al*. 2003]. With this fact in mind, the amplified undulation of vesicle membranes appeared to result from the addition of HRP.
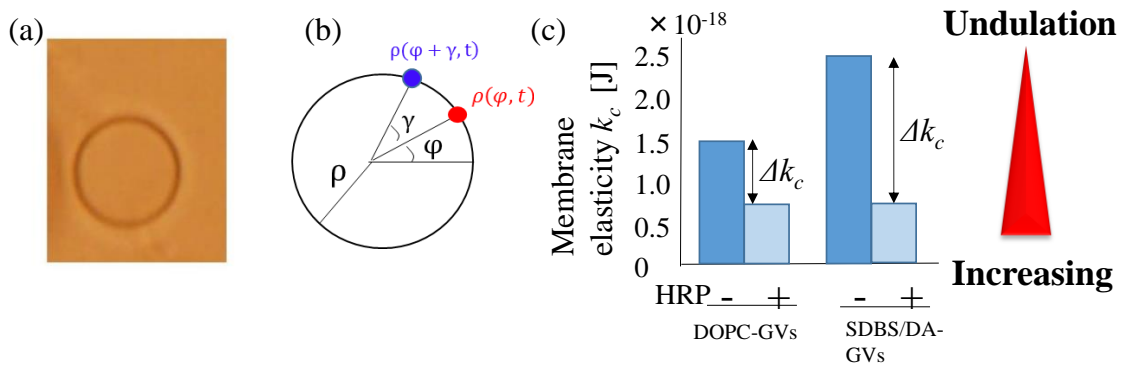


**Figure 2-5 Membrane elasticity of GVs with and without HRP (a) Example of GVs micrograph (DOPC) (b) Measurement method of membrane elastic coefficient (c) Comparison of $k_c$ value (entry 4, 9)**

**Table 2-3 Effect of HRP on membrane elasticity**

| entry | Lipid composition of GVs | $k_c \times 10^{18}$[J] | | $\Delta k_c \times 10^{18}$[J] |
|---|---|---|---|---|
| | | (-)HRP | (+)HRP | |
| 1 | NaH$_2$PO$_4$(no-GVs) | - | - | - |
| 2 | NaH$_2$PO$_4$/1,4-dioxane (1:1) (no-GVs) | - | - | - |
| 3 | POPC | 1.35 | 0.65 | 0.70 |
| 4 | DOPC | 1.54 | 0.66 | 0.88 |
| 5 | DOPG | 0.60 | 0.52 | 0.08 |
| 6 | Span20/Tween20 (75:25) | 1.62 | 1.55 | 0.07 |
| 7 | Span40/Tween40 (75:25) | 1.22 | 1.16 | 0.06 |
| 8 | Span80/Tween60 (75:25) | 1.08 | 0.80 | 0.28 |
| 9 | SDBS/DA (1:1) | 2.40 | 0.76 | 1.64 |
| 10 | SDBS/DA (75:25) | 2.18 | 0.81 | 1.37 |
| 11 | AOT | 2.08 | 0.81 | 1.27 |
| 12 | DOTAP | - | - | - |

### 3.6 Binding properties of HRP to lipid membranes

Another factor to induce the morphological change including the budding / fission of vesicles is the increase in surface area of outer leaflet of membranes. The above variation in excess surface can result from the protein-lipid membrane interaction such as the penetration and peripheral binding. Then, we measured the surface pressure-occupied area ($\pi$-$A$) isotherms that is a powerful approach to monitor the binding manner of proteins to the lipid monolayer.

The surface pressure ($\pi$) of SDBS/DA (50:50) (entry 9) was monitored with decreasing the occupied area $A$ as shown in Figure 2-6(a). The addition of HRP into the bulk aqueous phase shifted the $\pi$-$A$ isotherm to the higher $A$ range (**Figure 2-6 (a)**). The same was true for the case of SDBS/DA (75:25) (entry 10) and AOT (entry 11). The above results suggested that HRP penetrated into the monolayer of SDBS/DA or AOT. This implies that HRP was penetrated into the membrane interior of SDBS/DA- and AOT-GVs.

As shown in **Figure 2-6 (b)**, no shift of $\pi$-A isotherm by the addition of HRP was observed in the case of DOPC (entry 4). No shift of $\pi$-$A$ isotherm by HRP were also observed in the other lipid composition (entries 5-8) **Figure 2-6 (c)**. HRP was likely to bind to the surface of the above lipids.

We also examined the conformational change of HRP over its binding to the vesicle membrane by means of Trp fluorescence measurement. **Figure 2-6 (d)** shows no definite change in spectra with and without vesicles. That is, the binding process of HRP to the vesicle membrane would appear to induce no definite conformational change.
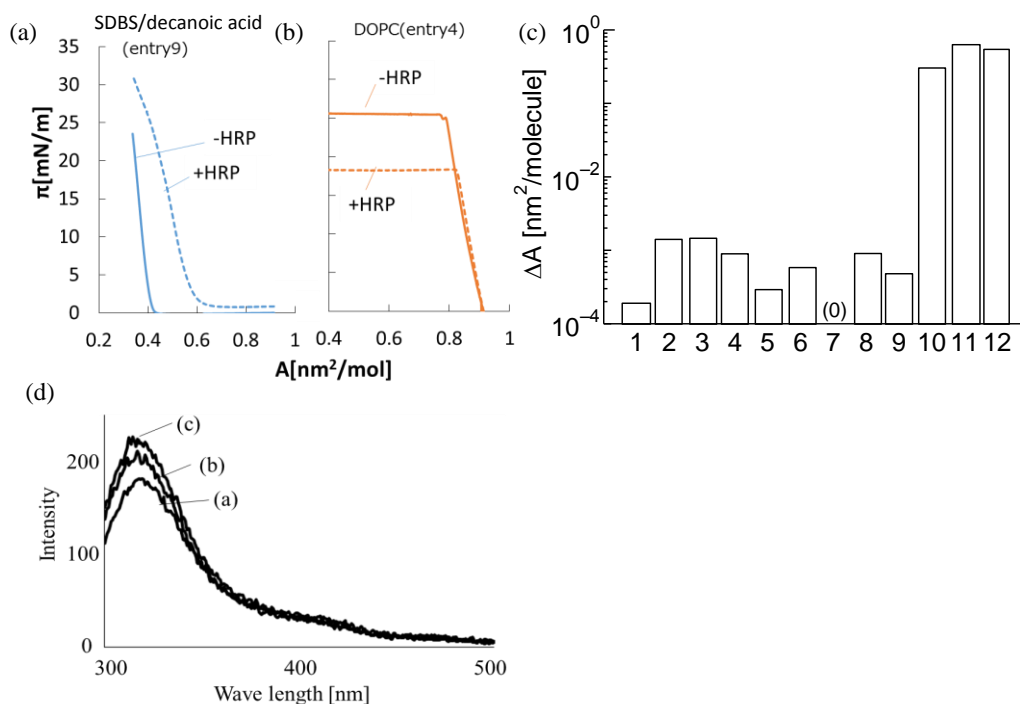
**Figure 2-6 Effect of HRP on π-*A* isotherm** for (a) SDBS/DA (entry 9) and (b) DOPC.(entry 4). (c) ΔA for each vesicle. (d) Tryptophan spectra for SDBS/DA (entry 9), DOPC (entry 4), and control condition.

## 3.7 Effect of Vesicle Composition on Degree of Polymerization of Polyaniline

To determine how the composition of the lipid membrane affects the degree of polymerization of polyaniline, the degree of polymerization of the product was measured using MALDI-TOFMS. The results of the obtained degree of polymerization are shown in **Figure 2-7**. When SDBS / DA-GVs were used, ES were polymerized, and the degree of polymerization was about $n \leqq 53$ (**Figure 2-7**). On the other hand, DOPC-GVs yielded PS with $n \leqq 17$. In each case, the degree of polymerization was higher than in the case without GVs, and it was suggested that the vesicle membrane had the effect of increasing the degree of polymerization in the polymerization reaction

of polyaniline. In addition, since ES has an H $^+$ charge, it was suggested that the polymerization may easily proceed particularly as a reaction field in the negatively charged SDBS / DA-GVs membrane. This suggests that a surfactant membrane having a strong negative charge may be a useful reaction field in ES polymerization.
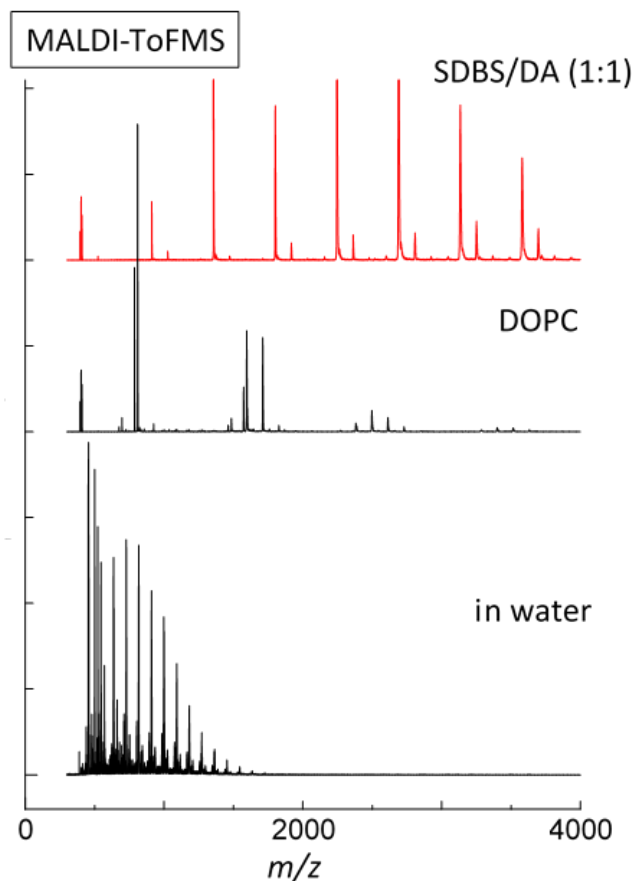


**Figure 2-7 MALDI-TOFMS spectra for each GV.**

## 3.8 Comparative study of selectivity with membrane instability

ES is an intermediate of PS in the polymerization reaction of aniline. According to the previous study, ES bears the positive charges due to its nature of bipolaron. Therefore, negatively charged GVs might capture ES on the vesicle surface. Thereby, the effect of net charge of GVs was assessed by using $\zeta$-potential. **Figure 2-8** shows the relationship between $\zeta$-potential of GVs and their reactivity. At around -100 mV of $\zeta$-potential, ES was likely to be produced relative to PS. In contrast, GVs with greater than -100 mV favored the production of PS. The same was true for the positively charged GVS (DOTAP; +75 mV).
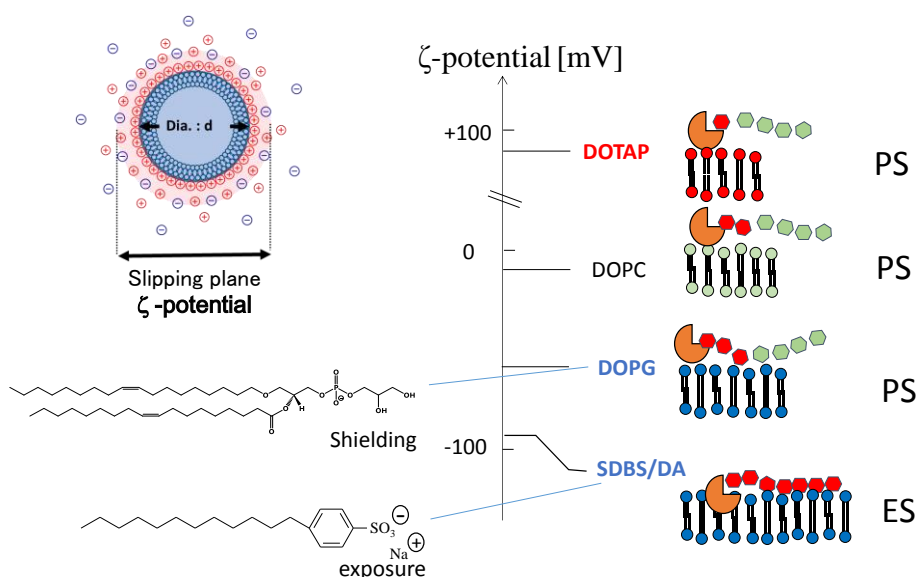


**Figure 2-8 Ladder of $\zeta$-potential for individual vesicle.**

To clarify the contribution of membrane dynamics to the template effect, the $\Delta A$ value was plotted against the corresponding $\Delta k_c$ value (**Figure 2-9 (a)**). The $\Delta A$ value increased at $\Delta k_c > 1 \times 10^{-19}$ J. The destabilizing effect by HRP is suggested to originate from the insertion of HRP into the lipid membrane. In contrast, the peripheral orientation of HRP was suggested at $\Delta k_c < 1 \times 10^{-19}$ J.

The $k_{1000}/k_{520}$ ratio that is an index for the selectivity of ES to PS was plotted against the corresponding $\Delta k_c$ value (**Figures 2-9 (b)**). Some vesicles (entries 3-8) indicated small $k_{1000}/k_{520}$ value in the lower $\Delta k_c$ range. In contrast, SDBS/DA- and AOT-GVs indicated the high $k_{1000}/k_{520}$ value in the higher $\Delta k_c$ range (entries 9-11). It was likely that the production of ES required a certain reduction of membrane elasticity. Alternatively, the $k_{1000}/k_{520}$ ratio was plotted against the corresponding $\zeta$-potential in **Figure 2-9 (c)**. This result suggested that the considerable negatively charged membranes afforded the production of ES.

From the diagram study regarding the reaction condition, the selectivity of ES to PS is likely to require the GV bearing both the membrane undulation property that the addition of HRP induces the large destabilizing effect to vesicle membranes ($\Delta k_c > 1 \times 10^{-19}$ J) and the negatively charged surface ($\zeta$-potential < -70 mV).
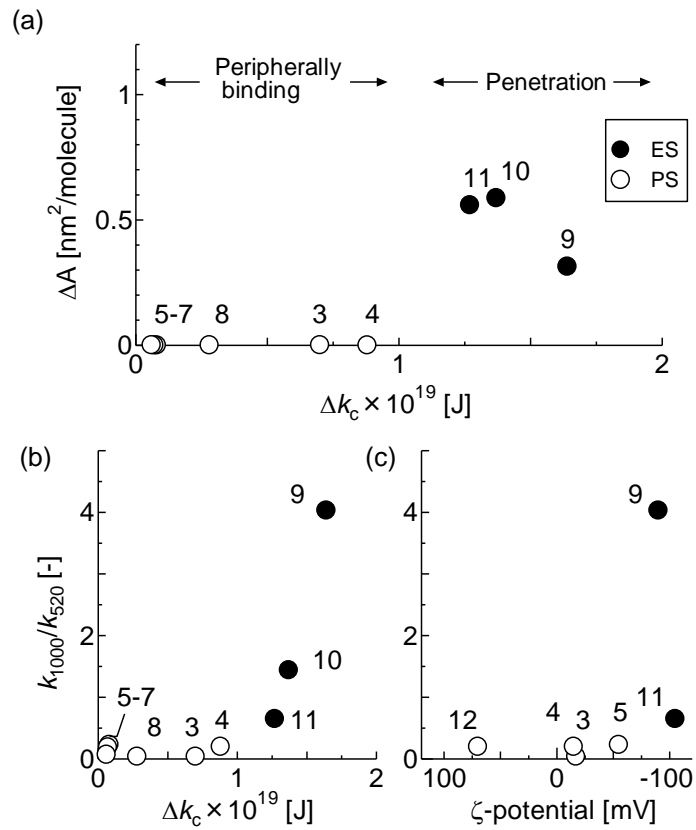
**Figure 2-9 Diagram of the reduction of membrane elasticity of GVs due to their interaction with HRP and their reactivity.** The number in figure represents entry shown in **Table 2-1**.

**4. Conclusion**

The author confirmed that GVs induced the template effect with respect to the polyaniline polymerization reaction, as well as vesicles with 100 nm in diameter. In the case of SDBS/DA-GVs, HRP was inserted into the vesicle membranes to induce their amplified undulation, which was advantageous for the production of ES. Besides, it was observed that the vesicle fission was accompanied with the polymerization reaction. In contrast, DOPC-GVs had no effect to induce both the production of ES and the morphological change of vesicles. By a comparison study, the coupling of polymerization reaction with the membrane undulation appeared to contribute to the reaction selectivity of polyaniline.

Meanwhile, the polyaniline polymerization at the surface of vesicle membranes induced their deformation and fission/budding as shown in **Figures 2-3 and 2-4**. These fission/budding should act as the obstacle against the application of vesicles to the sensor unit or drug delivery system. In the following Chapter, the author will address the suppression of membrane undulation enough to induce the fission/budding.

# References

Anagnostopoulos, A. A.; Alva, K. S.; Kumar J.; Tripathy, S. K., Biologically Derived Conducting and Water Soluble Polyaniline. *Macromolecules*, **31**, 4376-4378 (1998)

Cortese, J. D.; Schwab, B. 3rd.; Frieden, C.; Elson, E. L., Actin polymerization induces a shape change in actin-containing vesicles. *PNAS*, **86**, 5773-5777 (1989)

Erb, E.-M.; Chen, X.; Allen, S.; Roberts, C. J.; Tendler, S. J. B.; Davies, M. C.; Forsen, S., Characterization of the Surfaces Generated by Liposome Binding to the Modified Dextran Matrix of a Surface Plasmon Resonance Sensor Chip. *Anal. Biochem.,* **280,** 29-35 (2000)

Faucon, J.F.; Mitov, M. D.; Meleard, P.; Bivas, I.; Bothorel, P., Bending elasticity and thermal fluctuations of lipid membranes. Theoretical and experimental requirements. *J. Physique*, **50(17)**, 2389–2414 (1989)

Guo, Z.; R€uegger, H.; Kissner, R.; Ishikawa, T.; Willeke, M.; Walde, P., Vesicles as Soft Templates for the Enzymatic Polymerization of Aniline. *Langumuir*, **25(19)**, 11390–11405 (2009)

Heeger, A. J.; *Angew. Chem. Int. Ed*., **40**, 2591-2611 (2001)

W. Helfrich, *Z Naturforsch C.,* **11**, 693-703 (1973)

Himeno, H.; Shimokawa, N.; Komura, S.; Andelman, D.; Hamada, T.; Takagi, M., Charge-induced phase separation in lipid membranes. *Soft Matter*, **10**, 7959-7967 (2014)

Holopainen, J. M.; Angelova, M. I.; Kinnunen, P. K. J., Vectorial Budding of Vesicles by Asymmetrical Enzymatic Formation of Ceramide in Giant Liposomes. *Biophysical Journal,* **78**, 830-838 (2000)

Hub, H.H.; Zimmermann, U.; Ringsdorf., H., PREPARATION OF LARGE

UNILAMELLAR VESICLES. *FEBS Lett*, **140**, 254–256 (1982)

Jin, Z.; Su, Y.; Duan, Y., A novel method for polyaniline synthesis with the immobilized horseradish peroxidase enzyme. *Synthetic Metals,* **122**, 237-242 (2001)

Kaneda, Y., Virosomes: evolution of the liposome as a targeted drug delivery system. *Advanced Drug Delivery Reviews.,* **43,** 197-205 (2000)

Karami, H.; Mousavi, M.F.; Shampsipur, M., A new design for dry polyaniline rechargeable batteries. *J. Power Sources* **117**, 255-259 (2003)

Liu, W.; Cholli, A.L.; Nagarajan, R.; Kumar, J.; Tripathy, S.; Bruno, F. F.; Samuelson, L., The Role of Template in the Enzymatic Synthesis of Conducting Polyaniline. *J. Am. Chem. Soc*. **121**, 11345–11355 (1999)

Mita, N.; Tawaki, S.; Uyama, H.; Kobayashi, S., Enzymatic Oxidative Polymerization of Phenol in an Aqueous Solution in the Presence of a Catalytic Amount of Cyclodextrin. *Chemistry Letters,* 402-403 (2002)

Olea, D.; Viratelle, O.; Faure, C., Polypyrrole-glucose oxidase biosensor: Effect of enzyme encapsulation in multilamellar vesicles on analytical properties. *Biosens Bioelectron.,* **23,** 788-794 (2008)

Otero, T. F.; Martonez, J. G.; Pardilla, J. A., Biomimetic electrochemistry from conducting polymers. A review: Artificial muscles, smart membranes, smart drug delivery and computer/neuron interfaces. *Electrochimica Acta*, **84**, 112-128 (2012)

Peterlin, P.; Arrigler, V.; Kogej, K.; Svetinaa, S.; Walde, P., Growth and shape transformations of giant phospholipid vesicles upon interaction with an aqueous oleic acid suspension. *Chem. Phys. Lipids*, **159**, 67-76 (2009)

Phillips, M. C.; ChapMan, D., Monolayer characteristics of saturated 1,2-diacyl phosphatidylcholines (lecithins) and phosphatidylethanolamines at the air-water interface. *Biochim, Biophys. Acta.,* **23,** 301-313 (1968)

Shimanouchi, T.; Tasaki, M.; Vu, H. T.; Ishii, H.; Yoshimoto, N.; Umakoshi, H.: Kuboi, R., Aβ/Cu-catalyzed oxidation of cholesterol in 1,2-dipalmitoyl phosphatidylcholine liposome membrane. *J. Biosci. Bioeng*., **109**, 145-148 (2010)

Shimanouchi, T.; Kitaura, N.; Ohnishi, R.; Umakoshi, H.; Kuboi, R., Secondary nucleation of Aβ fibrils on liposome membrane. *AIChE J.*, **58**, 3625-3632 (2012)

Shimanouchi, T.; Umakoshi, H.; Kuboi, R., Growth Behavior of Giant Vesicles with Electroformation Method: Effect of Proteins on Swelling and Deformation. *J. Coll. Int'f Sci.*, **394**, 269-276 (2013)

Walde, P.; Umakoshi, H.; Stano P.; Mavelli, F., Emergent properties arising from the assembly of amphiphiles. Artificial vesicle membranes as reaction promoters and regulators. *Chem.Commun.,* **50,** 10177-10197 (2014)

Yanagisawa, M.; Imai, M.; Masui, T.; Komura, S.; Ohta, T., Growth Dynamics of Domains in Ternary Fluid Vesicles. *Biophysical journal*, **92(1)**, 115-125 (2007)

Zotti, G.; Cattarin, S.; Comisso, N., Cyclic potential sweep electropolymerization of aniline: The role of anions in the polymerization mechanism. *J. Electroanal. Chem*., **239**, 387-396 (1988)

# Chapter 3

# Evaluation of the effect of polymerization reaction on / in the membrane for vesicle destruction resistance due to vesicle membrane fluctuation

## 1. Introduction

Phospholipids and surfactants can form their molecular self-assemblies such as micelles or vesicles. The micelle is a thermodynamic equilibrium system formed under the condition where the lipid concentration surpasses the critical micellar concentration [Luisi, 2001]. In contrast, the vesicle that is a closed lipid bilayer is a thermodynamic (non-)equilibrium self-assembly system [Luisi 2001, Guida 2010]. The vesicle formation depends on the preparation method and the molecular characteristics such as the packing nature [Guida 2010, Walde 2004]. Therefore, the preparation method of vesicles has been widely studied [Walde 2004].

Vesicles composed of phospholipids have the biocompatible interface and has the capability to encapsulate the soluble or hydrophobic reagent [Luisi 2001, Guida 2010]. For these reasons, vesicles have been actively applied to the drug delivery system [Guida 2010]. Vesicles can also exert the catalytic property by using membrane compartment [Paprocki *et al*. 2015, Shimanouchi *et al.* 2010], act as the reaction field by functional ligands incorporated into the membrane as the reaction center [Umakoshi *et al*. 2008], and the separation field of target materials [Jesorka nd Orwar,2008]. The further application of vesicles is its use as a platform to mimic the bio-function; the artificial cell system [Hamada *et al*. 2005, Elani *et al*. 2018]. The optimal diameter of vesicles for the aforesaid applications is at most 100 nm. This is because vesicles with

sub-micron size in diameter, relative to ones with micron size, are advantageous for the reaction / separation field in terms of their large surface-to-area. Thus, vesicles with sub-micron size in diameter has been strongly demanded in the practical application aspects.

However, it is well-known that the vesicle membranes sometimes deform and bud by the strong undulation accompanied with the outer stimuli [e.g. Terasawa *et al*. 2012]. In actual, the polymerization reaction also acted as the outer stimuli as presented at the last Chapter. For the application of vesicles to sensor unit or reaction/separation fields, the stable membrane structure with keeping the flexibility to the outer stimuli would be required.

The suppression of membrane undulation has been highly developed in the biosystem. **Figure 3-1** shows the lining structure of biomembranes. This structure is constructed by the cytoskeltons that is the polymerized proteins (actin fillaments [Kotila *et al*. 2019]). For the effective construction of lining structure, the cytoskeltons are localized on the microdomains on biomembranes [Szymanski *et al*. 2015]. The biomembrane interacts with the outer stimuli such as the proteins and small-sized compounds. Biomembranes up-take these compounds by the manner called as "endocytosis". This phenomenon is driven by the deformation of membranes. The step to require the membrane deformation and fission/budding such as endocytosis is advanced by avoiding the region of cytoskeltons. In contrast, the maintenance of morphology utilizes the cytoskeltons. To induce the indispensable functions for the biosystem, these phenomena are collaborated with controlling the polymerization / depolymerization of proteins as the constituent of cytoskeletons.

| Deformation of biomembranes | Biomembrane with lining structure |
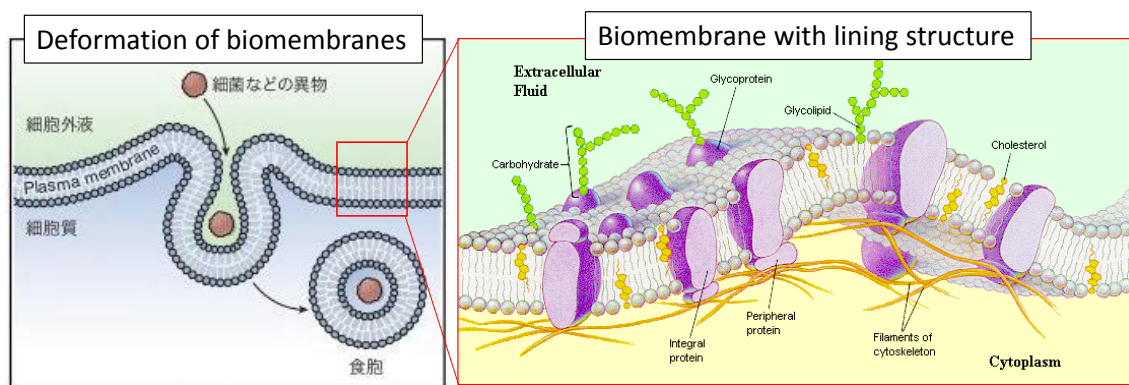
**Figure 3-1 Structure of biomembranes.** (Left) Deformation of biomembranes to the external factor. (Right) Lining structure of biomembranes.

To reinforce the vesicle structure against the strong undulation due to the external force, the following strategies would be promising:

(1) Polymerization reaction at the surface

(2) Polymerization reaction at the interior of vesicle membrane

(3) Lining structure.

In Chapter 3, the author studied the approaches (1) and (2) because the approaches (3) is still now difficult under the present situation concerning the techniques of vesicles. First, the vesicle embedded with hydrophilic polymers was prepared for the approach (1). 1,2-Dimyristoyl-sn-glycero-3-phosphocholine (DMPC) was used to prepare the vesicle because DMPC vesicle indicated no cytotoxicity [Funamoto *et al*. 2009]. PVP was mainly used as a hydrophilic polymer. For a comparison study, *isotactic*-poly(methylmethacrylate) (*iso*-PMMA), *syndiotactic*-poly(methylmethacrylate) (*syn*-PMMA), and poly-L-lactic acid were used. The morphology of vesicles were then observed with a cryo-TEM. The effect of polymer coverage was investigated based on the calcein leakage. For the approach (2),

42

the author tried the photopolymerization of phospholipids. The effect of polymerization

time on the membrane structure was examined in terms of calcein leakage.

## 2. Materials and Methods

### 2.1 Materials

The lipids and reagents used were 1,2-dioleoyl-sn-glycero-3-phosphocholine (DOPC), decanoic acid (DA), peroxidase from horseradish (HRP), $CoCl_2$ were purchased from Wako Pure Chemicals Ltd (Osaka, Japan). 1,2-dipalmitoyl-*sn*-glycero-3-phosphocholine (DPPC), 1,2-dimirystoyl-*sn*-glycero-3- phosphocholine (DMPC), sodium dodecylbenzene sulfonate (SDBS) were purchased from Tokyo Chemical Industry Co., Ltd. (Tokyo, Japan). sepharose 4B, and Triton X-100 were purchased from Sigma-Aldrich Japan (Tokyo, Japan). Calcein was purchased from Dojindo (Kumamoto, Japan).

### 2.2 Preparation of vesicles

Vesicles were prepared according to the previous method [MacDonald *et al*., 1991, Manosroi *et al*., 2003, Guo *et al*., 2009 ]. Phospholipids and Surfactants were dissolved in a chloroform solution (10 mg/mL). To prepare the PVP composite vesicle, a mixture of 5 wt% of PVP was dissolved in a chloroform solution (10 mg/mL). The organic solvent was removed by evaporation in a rotary evaporator. The residual lipid film, after drying under a vacuum overnight, was hydrated with the 100 mM calcein solution to form multilamellar liposomes (MLVs). For the preparation of unilamellar vesicles by extrusion, the MLV suspension was subjected to five cycles of freezing and thawing, and passed 15-times through two stacked polycarbonate filters with 100 nm pores (Nuclepore, Costar, Cambridge,MA) at room temperature by using an extrusion device (Liposofast; Avestin Inc.). To prepare vesicles entrapping calcein, free calcein was removed by a gel permeation chromatography (Sepharise 4B, φ 15mm, height 150

mm).

## 2.3   Preparation of photopolymerizable lipid vesicles

Vesicles were prepared according to the previous method [MacDonald *et al*., 1991, Manosroi *et al*., 2003, Guo *et al*., 2009]. The photopolymerizable lipid was mixed at a ratio of 1: 1 based on the existing method [Chun *et al*., 2018]. After the vesicle preparation, UV (254 nm) was irradiated for a predetermined time to polymerize the lipid membrane with a Handy UV Lamp (SLUV-4; ASONE).

## 2.4 Microscopic observation

The vesicles were rapidly frozen in liquid ethane and the morphology of the vesicles was observed using a transmission electron microscope (cryo-TEM). Some samples were subjected to TEM observation by negative staining.

## 2.5 Calcein leakage assay

A calcein leakage experiment was performed according to the previous literatures [Kuboi *et al*., 2004, Shimanouchi *et al*., 2013]. The vesicles entrapped calcein were prepared with a hydration method. In short, a lipid film was hydrated with calcein solution (100 mM). Size exclusion chromatography was performed to remove calcein not entrapped. Calcein-encapsulated vesicles (250 μM) and proteins (10 μM) were mixed, and the fluorescence intensity was measured at an excitation wavelength of 490 nm and a emission wavelength of 520 nm with a fluorescence spectrophotometer (FP6500). Finally, Triton-X 100 was added to disrupt the vesicles, and the maximum fluorescence intensity was measured to obtain the calcein leak rate *RF* value.

$$RF = 100 \times (I(t)\text{-}I_0)/(I_{\text{total}}\text{-}I_0) \ (\%) \qquad\qquad \textbf{(3-1)}$$

$I(t)$ is the intensity at time $t$, and $I_0$ and Itotal are the intensities immediately after the start of the release analysis and immediately after the addition of Triton X-100, respectively. First-order kinetics were employed to analyze calcein release:

$$RF(t) \ = \ RF_{\text{max}}(1\text{-}\exp(\text{-}kt)) \qquad\qquad \textbf{(3-2)}$$

$RF_{\text{max}}$ and $k$ represent the maximum value of $RF$ and the release rate constant, respectively. To determine $RF_{\text{max}}$, all experiments were run until the value of calcein fluorescence reached a constant value.

In a calcein leakage experiment of vesicles prepared with photopolymerizable lipids, a cobalt quenching method was used [Kendall and Macdonald, 1983]. Since calcein has a property of being quenched by forming a complex with cobalt, calcein fluorescent molecules leaked to the outside can be quenched by adding a equimolar amount of a cobalt chloride solution to a vesicle solution.The fluorescence intensity was measured over time using a fluorescence spectrophotometer (FP-8200, manufactured by JASCO) while shaking with a constant temperature shaker. The excitation wavelength is 490 nm and the emission wavelength is 520 nm.Finally, Triton-X was added to destroy the liposome, and the fluorescence intensity was measured. The leak rate was calculated by the following equation.

$$RF = 100 \times (I_0 \text{ - } I(t))/(I_0) \ (\%) \qquad\qquad \textbf{(3-3)}$$

## 2.6 Giant vesicle (GVs) Preparation

The lipid was dissolved in chloroform, and the lipid membrane was placed in a round-bottom flask using an evaporator. After allowing to stand overnight, giant vesicles (GVs) were prepared by allowing them to stand in a constant temperature bath at 70 °C. for 4 hours by the high-temperature hydration method [Hub *et al*. 1982]. A dispersion with an average particle size of about 10 µm and a concentration of 10 mM was prepared.

## 2.7 Measurement of membrane elastic modulus by membrane fluctuation analysis

The fluctuation of the film was discussed by measuring the film elastic coefficient $k_c$ according to the previous method [Faucon *et al*. 1989]. Briefly, using the radius $\rho(\varphi, t)$ of the vesicle at a certain time $t$ and the radius $\rho(\varphi + \gamma, t)$ at a position shifted by an angle therefrom, the correlation function $\xi(\gamma, t)$ can be defined. Using the time average $\xi(\gamma)$ of $\xi(\gamma, t)$, the membrane elastic coefficient $k_c$ can be obtained from **equation (3-5)**.

$$\xi(\gamma, t) = \frac{1}{R^2}\left[\int_0^{2\pi} \rho(\varphi + \gamma, t)\rho(\varphi, t)d\varphi - \rho^2(t)\right] \quad \textbf{(3-4)}$$

$$\xi(\gamma) = <\xi(\gamma, t)> = \frac{kT}{4\pi k_c}\sum_{n=2}^{n_{max}} f(n, \sigma)P_n(cos\gamma) - (Correction\ term) \ \textbf{(3-5)}$$

$R$ is the vesicle radius. $f(n, \sigma)$ is a function of natural number $n$ and membrane tension $\sigma$, and $P_n(x)$ is a Legendre polynomial. The effect of the focus of the objective lens deviating from the true center of the vesicle was corrected by the correction term in **equation (3-5)**.

## 3. Results and Discussion

### 3.1 Cryo-TEM observation of vesicles

In the first series of experiments, a cryo-TEM observation was performed to confirm the morphology of vesicles prepared by using phospholipids and surfactants. **Figure 3-2** shows the representative cryo-TEM images for individual vesicles. DMPC vesicles were spherical shape. Other DMPC vesicle modified with polymers indicated non-spherical shape such as prolate and stomatocyte (a part of the sphere is dented), as shown in **Figure 3-2 (b)-(e)**. Interestingly, DMPC/PVP vesicles stacked each other without fusion (**Figure 3-2 (f)**). This possibly resulted from the bridge of fully hydrated PVP between vesicles. Those deformation of polymers is driven by the volumetric reduction process as shown in **Figure 3-3**.
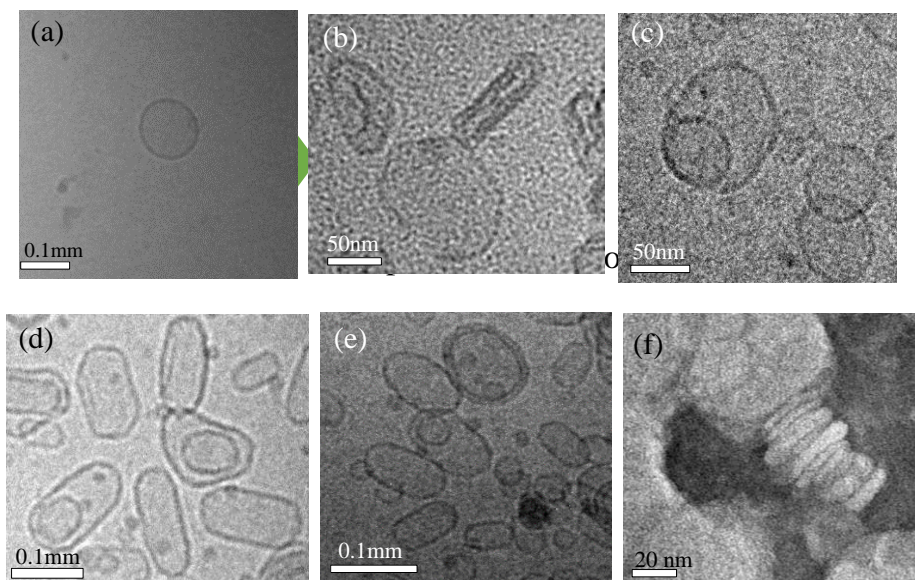


**Figure 3-2 Cryo-TEM images** on DMPC (a) unmodified and modified with (b)DMPC/PVP, (c)DMPC/PLLA, (d)DMPC/*iso*-PMMA, (e)DMPC/*syn*-PMMA. (f) Negative stained TEM image of DMPC/PVP.
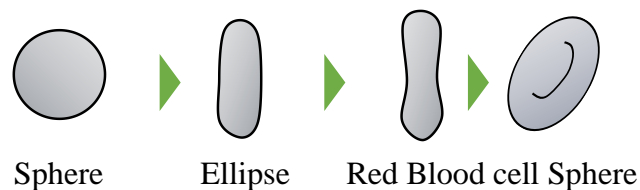
Sphere     Ellipse     Red Blood cell Sphere

**Figure 3-3 Morphological change of liposomes due to the osmosis difference. Water flow from inner to outer aqueous phase was induced by the osmosis difference across the vesicle membrane.**

## 3.2 Calcein leakage

### 3.2.1    Effect of the coverage by hydrophilic polymers

Calcein leakage behavior of DMPC vesicles modified with PVP next examined. **Figure 3-4** shows the time-course of calcein leakage amounts, *RF*, estimated from its fluorescence intensity. The modification of PVP obviously increased the RF value. Therefore, it was suggested that the vesicle deformation accompanying the addition of PVP promoted the leakage. Next, HRP was added to monitor the calcein leakage. No significant change in the time-course of RF value was observed between bare- and PVP-modified DMPC vesicles. This strongly suggested that the PVP could suppress the membrane undulation with keeping the interaction of membranes with HRP.
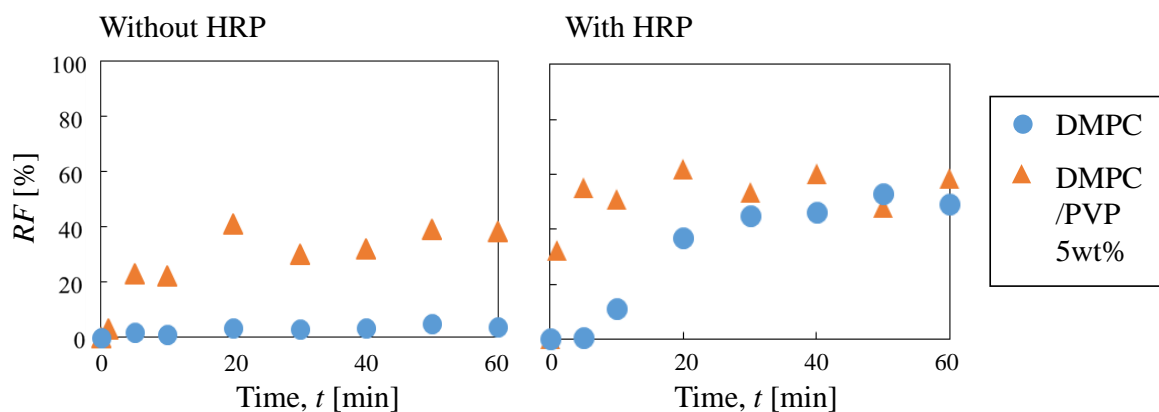


**Figure 3-4 The time-course of *RF* for PVP-modified DMPC liposome with and without HRP.**

49

## 3.2.2 Effect of photopolymerization of lipids in vesicle membranes

To clarify the influence of polymerization extent, the calcein leakage was examined with varying the polymerization time. The polymerization time that is a treatment time of UV at 254 nm was set between 0 and 120 minutes. Afterwards, HRP was mixed with the UV-treated vesicles. **Figure 3-5** shows the time-course of $RF$ values for individual vesicles (un)treated with UV. Under no UV irradiation, the trend of $RF$ value was almost identical with and without HRP (**Figure 3-5 (a)**). The same was true for the vesicles treated with UV irradiation for 60 and 120 minutes (**Figures 3-5 (b) and (c)**. Furthermore, the maximal $RF$ value, $RF_{max}$ was plotted as a function of UV irradiation time as shown in **Figure 3-5 (d)**. The addition of HRP to vesicles resulted in no significant difference in $RF_{max}$ nevertheless to the irradiation time of UV.
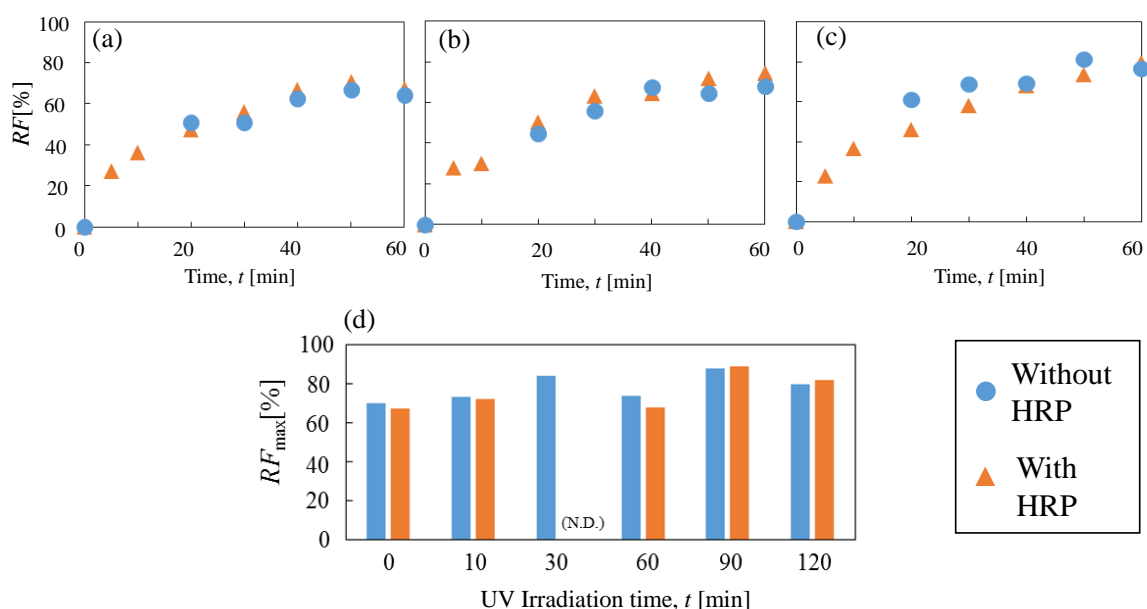


**Figure 3-5 The time-course of $RF$ for DPPC/DiynePC(2:1) vesicle with and without HRP.** (a) 0, (b) 60, and (c)120 min. (d) Comparison of $RF_{max}$ with and without HRP in DPPC/DiynePC(2:1) vesicles (un)treated with UV irradiation.

## 3.3 Effect of HRP addition on membrane elasticity of GVs

For each vesicle, the change in membrane elastic modulus $k_c$ ($\Delta k_c$) when HRP was added was measured (**Table 3-1**). DMPC vesicles modified with PVP did not show much change even after the addition of HRP. This suggests that the morphological change due to the modification by PVP occurred before the addition of HRP, and that the change in membrane elastic modulus caused by the addition of HRP was small. This result is consistent with the fact that calcein leaked before HRP addition, as shown in 3.2.1. In the DPPC / DiynePC (2: 1) vesicles without UV irradiation, it was suggested that the membrane fluctuation occurred by adding HRP. For DPPC / DiynePC (2: 1) vesicles that had been irradiated with UV, the results showed that the membrane elastic modulus was increased by the addition of HRP. This suggests that DPPC / DiynePC (2: 1) vesicles exhibit a large hole in the lipid membrane due to photopolymerization, indicating a different leakage mechanism from other vesicles.

**Table 3-1 Effect of HRP on membrane elasticity**

| Lipid composition of GVs | $k_c \times 10^{18}$[J] | | $\Delta k_c \times 10^{18}$[J] |
|---|---|---|---|
| | (-)HRP | (+)HRP | |
| DMPC/PVP(5wt%) | 0.21 | 0.24 | -0.03 |
| DPPC/DiynePC(2:1) (No UV light irradiation) | 1.72 | 0.51 | 1.21 |
| DPPC/DiynePC(2:1) (UV light irradiation) | 0.51 | 0.72 | -0.21 |

## 3.4 Effect of surface polymerization of polyaniline

From the results of Chapter 2, polyaniline polymerization occurs on the surface of vesicle membranes because the localization of HRP molecule is likely to be at the surface of vesicle membrane. The detailed findings are consulted in Chapter 4. Besides, perngraniline salts are likely to be released from the HRP on the vesicle membranes to the bulk aqueous phase. In contrast, AOT- and SDBS/DA(1:1) vesicles could capture emelardine salts as the intermediate. However, the polymerization extent was at most 50, which was too low as compared with that of PVP (Mw. ~ 1,000 kDa). It was therefore considered that the vesicles modified with emeraldine salts made it difficult to apply to other usages including the sensor unit.

## 4. Conclusion

The author considered three possible approaches. First, the coverage of hydrophilic polymer was tested by using several kinds of polymers. Of these polymers, PVP succeeded in the coverage without the disruption of vesicles. For the reason, to reinforce the resistance to membrane disruption is expected. The second approaches is the polymerization of constituent phospholipids of vesicles. The calcein leakage experiments indicated no impact of photopolymerization of phospholipids in liposomal membranes on the membrane structure. Besides, no impact on HRP addition was confirmed. Therefore, this approach was not available for the suppressed effect of membrane undulation. Thus, the remaining approaches is the third one, that is, the lining structure of vesicle membranes as mimicking biomembranes. In the present study, this approach was not studied because of the difficulty. It is noted that the biomembrane has applied the lining structure including cytoskeleton. From these findings, the construction of the lining structure to the vesicle membranes would be promising approach that is the reinforcement of membrane structure against the strong undulation enough to result in the membrane disruption.

# References

Chun, M. J.; Choi, Y. K.; Ahn, D. J., Formation of nanopores in DiynePC–DPPC complex lipid bilayers triggered by on-demand photo-polymerization. *the Royal Society of Chemistry*, **8**, 27988-27994 (2018)

Elani, Y.; Trantidou, T.; Wylie, D.; Dekker, L.; Polizzi, K.; Law, R. V.; Ces, O., Constructing vesicle-based artificial cells with embedded living cells as organelle-like modules. *Sci. Rep*., **8**, Article number 4564 (2018)

Funamoto, K.; Ichihara, H.; Matsushita, T.; Matsumoto, Y.; Ueoka, R., Marked therapeutic effects of hybrid liposomes on the hepatic metastasis of colon carcinoma. Y*AKUGAKU ZASSHI* **129(4)**, 465-473 (2009)

Guida, V., *Adv. Coll. Int'f. Sci*., **161**, 77-88 (2010)

Guo, Z.; R€uegger, H.; Kissner, R.; Ishikawa, T.; Willeke, M.; Walde, P., Vesicles as Soft Templates for the Enzymatic Polymerization of Aniline. *Langumuir*, **25**(19), 11390–11405 (2009)

Hamada, T.; Sato, Y. T.; Yoshikawa, K.; Nagasaki, T.; Reversible photoswitching in a cell-sized vesicle. *Langmuir*, **21**, 7626-7628 (2005)

Jesorka, A.; Orwar, O., Liposomes: technologies and analytical applications. *Ann. Rev. Anal. Chem*., **1**, 801-832 (2008)

Kendall, D. A.; Macdonald, R. C., Characterization of a fluorescence assay to monitor changes in the aqueous volume of lipid vesicles. *Analytical Biochemistry*, **134,** 26-33 (1983)

Kotila, T.; Wioland, H.; Enkavi, G.; Kogan, K.; Vattulainen, I.; Jégou, A.; Romet-Lemonne, G.; Lappalainen, P., Mechanism of synergistic actin filament pointed end depolymerization by cyclase-associated protein and cofilin. *Nature*

*Comm*. **10**, Article ID 531 (2019)

Kuboi, R.; Shimanouchi, T.; Yoshimoto, M.; Umakoshi, H., Detection of Protein Conformation under Stress Conditions Using Liposomes As Sensor Materials. *Sensors and Materials*, **16**, 241-254 (2004)

Luisi, P. L.; Are micelles and vesicles chemical equilibrium systems. *J. Chem. Educ*., **78**, 380-384 (2001)

MacDonald, R. C.; MacDonald, R. I.; Menco, B. Ph. M.; Takeshita, K.; Subbarao, N. K.; Hu, L., Small-volume extrusion apparatus for preparation of large, unilamellar vesicles. *Biochim. Biophys. Acta.,* **1061**, 297-303 (1991)

Manosroi, A.; Wongtrakul, P.; Manosroi, J.; Sakai, H.; Sugawara, F.; Yuasa, M.; Abe, M., Characterization of vesicles prepared with various non-ionic surfactants mixed with cholesterol. *Colloid. Surface B*., **30** 129-138 (2003)

Paprocki, D.; Koszelewski, D.; Walde, P.; Ostaszewski, R., Efficient Passerini reactions in an aqueous vesicle system. *RSC Adv*., **5(124)**, 102828- 102835 (2015)

Shimanouchi, T.; Tasaki, M.; Vu, H. T.; Ishii, H.; Yoshimoto, N.; Umakoshi, H.: Kuboi, R., Aβ/Cu-catalyzed oxidation of cholesterol in 1,2-dipalmitoyl phosphatidylcholine liposome membrane. *J. Biosci. Bioeng*., **109**, 145-148 (2010)

Shimanouchi, T.; Nishiyama, K.; Hiroiwa, A.; Vu, H. T.; Kitaura, N.; Umakoshi, H.; Kuboi, R., Growth Behavior of A β Protofibrils on Liposome Membranes and Their Membrane Perturbation Effect. *Biochem. Eng. J*., **71**, 81-88 (2013).

Szymanski, W. G.; Zauber, H.; Erban, A.; Gorka, M.; Wu, X. N.; Schulze, W. X., Cytoskeletal Components Define Protein Location to Membrane Microdomains. *Mol Cell Proteomics*., **14(9)**, 2493–2509 (2015)

Terasawa, H.; Nishimura, K.; Suzuki, H.; Matsuura, T.; Yomo, T., Coupling of the fusion and budding of giant phospholipid vesicles containing macromolecules. *PNAS*, **109 (16)**, 5942-5947 (2012)

Umakoshi, H.; Morimoto, K.; Ohama, Y.; Nagami, H.; Shimanouchi, T.; Kuboi, R., Liposome Modified with Mn−Porphyrin Complex Can Simultaneously Induce Antioxidative Enzyme-like Activity of Both Superoxide Dismutase and Peroxidase. *Langmuir*, **24**, 4451-4455 (2008)

Walde, P., *Encycl. Nanosci. Nanotechnol.*, **9,** 43-79 (2004)

# Chapter 4
# Effect of vesicle membrane fluctuation on protein adsorption

## 1. Introduction

Phospholipid- and surfactant vesicle are a promising material for an artificial cell [Elani *et al*., 2014], reactor [Elani *et al*., 2014, Bolinger *et al*., 2004, Nomura *et al*., 2003], biosensor unit [Kuboi *et al*., 2004, Fukuma *et al*., 2017, Zhang *et al*., 2016], or vehicle in the drug delivery [Hayashi *et al*., 2017]. These possible applications originate from the compartment effect [Nomura *et al*., 2003] and self-assembled structures [Barauskas *et al*., 2005]. Besides, the vesicle system can be regarded as a kind of W/O/W emulsion system [Umakoshi *et al*., 2013]. Such nature of the vesicle system can achieve a simple chemical process with less consumption of energy and material. Therefore, the vesicle system can act as a (bio)separation field [Kuboi *et al*., 2004, A. Fernández and Berry 2003, Jesorka and Orwar, 2008] and designable reaction field [Umakoshi *et al*., 2013].

For an efficient usage of vesicles, the clarification of the partition mechanism of target materials including small (bio)molecules and proteins to vesicle membranes is an important issue in the biophysical and engineering aspects. Investigations regarding the partitioning behavior of small (bio)molecules have been widely studied as compared with proteins [Umakoshi *et al*., 2013, Kupiainen *et al*., 2005]. Proteins are in general categorized into soluble proteins and membrane proteins. The partition behavior of membrane protein originates from the amino acid sequence [Wimley *et al*., 1996]. Hydrophobic regions on the secondary structure of protein favors the hydrophobic region of lipid membranes to be partitioned. Alternatively, the partition

behavior of soluble proteins depends on their conformation and property of lipid membranes by using small-sized proteins (at most 30 kDa) [Shimanouchi *et al*., 2014, Hitz *et al*., 2006] and antimicrobial / cell-penetrating peptides [Almeida *et al*., 2009]. The headgroup mobility on the surface of vesicle membranes generates a hydrophobic crevice/pothole [Shimanouchi *et al*., 2011], which is a platform for the binding of small-sized proteins [Shimanouchi *et al*., 2014]. Meanwhile, the possibility that this scenario mentioned above can be applied to soluble proteins with high molecular weight is still unclear.

In line with this, horseradish peroxidase (HRP) is a good example for the middle-sized protein as a model system other than serum albumin from human or bovine (66.5 kDa), from the viewpoints of its functionality and possible partitioning property. HRP has the molecular weight of about 40 kDa and its polypeptide chain of 308 amino acids folds to 13 a-helices and three b-sheets [Gajhede *et al*., 1997]. The proper HRP conformation is stabilized by four disulfide bonds [Zakharova *et al*., 2011]. In addition, the catalytic property of HRP has been well-known in several reviews [Zakharova *et al*., 2011, Veitch 2004, Ryan *et al*., 2006]. In particular, the catalytic action of HRP on the vesicle surface is considered as a key step for a reaction selectivity of polyaniline polymerization [Guo *et al*., 2009].

Therefore, a clarification of the partition behavior for middle-sized protein HRP would result in two important suggestions: a possibility whether a scenario obtained by using small-sized proteins can be applied to the middle-sized proteins and a deeper understanding on the HRP-catalyzed polymerization reaction of polyaniline to control its selectivity.

In Chapter 4, the binding characteristics of the target protein HRP to vesicle

membranes was investigate. According to previous studies, negatively charged surfactant vesicles composed of sodium di-2-ethylhexylsulfosuccinate (AOT) and sodium dodecylbenzene sulfonate (SDBS) / decanoic acid (DA) (mixing ratio 1 : 1) were used because these surfactant vesicles indicated the strong interaction with HRP [Guo *et al*., 2009]. Two zwitterionic phospholipids 1,2-dioleoyl-*sn*-glycero-3-phosphocholine (DOPC) and 1,2-dimirystoyl-*sn*-glycero-3-phosphocholine (DMPC) were used as a control system to surfactant vesicles. The interaction between HRP and vesicles was examined from two approaches: a calcein leakage experiment [Kuboi *et al*., 2004, Fukuma *et al*., 2017, Shimanouchi *et al*., 2009] and quartz crystal microbalance method [Vu *et al*., 2009]. This is because the calcein leakage can be an quantitative index for the extent of HRP-vesicle interaction and give the implication for the change in membrane structure by HRP. The QCM study can measure the adsorbed mass of HRP as the quantitative index for the HRP-vesicle interaction. The partition property of HRP, resulting in the HRP-vesicle interaction, was analyzed with a thermodynamic model, surface pressure isotherms and dielectric measurement. The possible partitioning mechanism of HRP to vesicle membranes was finally discussed.

## 2. Materials and Methods

### 2.1 Materials

The lipids and reagents used were 1,2-dioleoyl-*sn*-glycero-3-phosphocholine (DOPC), decanoic acid (DA), and HRP from horseradish were purchased from FUJIFILM Wako Pure Chemical Corporation  (Osaka, Japan). 1,2-dimirystoyl-*sn*-glycero-3-phosphocholine (DMPC), sodium dodecylbenzene sulfonate (SDBS), and sodium di-2-ethylhexylsulfosuccinate (AOT) were purchased from Tokyo Chemical Industry Co., Ltd. (Tokyo, Japan). Calcein was purchased from Dojindo (Kumamoto, Japan). Other chemical reagents were of analytical grade.



**Scheme 4-1 Chemical structure of lipids used here.** (a) DOPC, (b) DMPC, (c) SDBS, (d) DA, (e) AOT.

## 2.2 Preparation of vesicles

A vesicle with a particle size of 100 nm was prepared according to the conventional method [Shimanouchi *et al*., 2011]. The lipid mixture was dissolved with chloroform in a round-bottom flask, and chloroform was removed by an evaporator to form a lipid thin film. Drying process was performed overnight under vacuum to remove all remaining solvent. The dried lipid film was thereafter hydrated by 50 mM Tris HCl solution (pH7.5) including 100 mM NaCl to obtain a total lipid concentration of 10 mM and final volume of 3 mL. Multilayer vesicles were prepared by the freeze-thaw method. Thereafter, vesicles having a uniform particle size of 100 nm were prepared by the extrusion method. These vesicles were observed by a cryo-TEM to confirm their morphology.

## 2.3 Lipid planar membrane formation

Quartz crystal unit (BAS, crystal unit Au) was immersed in a 1-decanethiol / ethanol solution (2 mM) to form a thiol self-assembled film. A thiol self-assembled monolayer is a type of self-assembled monolayer (SAM), which is a self-assembled monolayer that is formed spontaneously when a substrate is immersed in a solution. In addition, it is thought that this membrane can easily obtain a highly oriented monomolecular film and show high stability, so that it is easy to form a lipid membrane with high alignment on the substrate. Next, the substrate was immersed in a lipid / chloroform solution (10 mM), dried, washed with water, and dried to form a planar lipid membrane.

## 2.4 Quartz crystal microbalance (QCM) method

Based on the previous method [Vu *et al*., 2009], the adsorbed amount of HRP to lipid membranes was measured with the QCM combined with the immobilization technique of lipid membrane. The QCM electrode (Au electrode) was immersed in an ethanol solution (1 mM) containing 11-mercaptonecanoic acid (MUA) for 12 hours to form a thiol self-assembled membrane (SAM) on the gold surface. After drying and washing of the SAM on electrode, the SAM-based electrode was exposed for 4 hours to 17 mM each of *N*-hydroxysuccinimide (NHS) and *N*-(3-dimethyl aminopropyl)-N-ethylcarboimide hydrochloride to activate the terminal carboxy group. The NHS-activated SAM on electrode was dried, thereafter, coupled to an ALS / CHI electrical microbalance quartz crystal (400, BAS Inc.). The amino group-doped (PE: 2 mol% content) vesicle suspension (5 mL) was loaded for 1 hour to the electrode for its immobilization.

According to Sauerbrey's equation (**Equation (4-1)**), there is a linear relationship between the decrease in frequency ($-\Delta f$) and the increase in mass per unit area ($\Delta m/A$).

$$\Delta f = -\frac{2 f_0^2}{\sqrt{\mu \rho}} \frac{\Delta m}{A} \qquad \textbf{(4-1)}$$

where $\Delta m$, $f_0$, $A$, $\mu$, and $\rho$ represents mass change, fundamental frequency, electrode area Shear stress of quartz, and Amber quartz density, respectively.

## 2.5 Surface pressure analysis

Surface pressure analysis was performed to determine the π-A isotherm, and protein orientation analysis was performed by Small LB film making device FSD-220C (U.S.I Corp.) and LB LIFT CONTROLLER FSD-23(U.S.I Corp.) according to Chapter2. First, 60 μL of lipid (1 mM) dissolved in chloroform was dispersed in a water tank filled with ultrapure water. After allowing the lipid to stand at the gas-liquid interface for 15 minutes, pressure was applied to the surface with a barrier to investigate the change in occupied area (*A*) due to the change in the surface pressure (π). Lipid was dispersed and allowed to stand for 15 min, then 60 μL of protein solution (HRP: 5 mg / mL) was added to the water bath, after 5 min left, Similarly, changes in *A* due to changes in π were investigated, and the orientation pattern of proteins was discussed from the curve change due to the presence or absence of protein.

## 2.6 Dielectric dispersion analysis

In order to analyze the relaxation behavior derived from the microscopic motion of the lipid molecule assembly interface, we used a coaxial cell with an RF impedance analyzer (Agilent 4291B RF impedance / material ・analyzer, Agilent Technologies), according to the previous method [Shimanouchi *et al*., 2011].The calibration was performed by using open, short, and load mode. Thereafter, the cell constant $C_0$ was determined by using water, methanol, and ethanol. The sample was packed into the electrode, and the capacitance $C_p$ and conductivity $G$ were measured at a frequency of 1 MHz to 1 GHz, and the relative permittivity ε 'and dielectric loss ε' were calculated from the following equations:

$$\varepsilon' = \frac{C_p}{C_0} \qquad \textbf{(4-2)}$$

$$\varepsilon'' = \frac{G - G_0}{2\pi f C_0} \qquad \textbf{(4-3)}$$

where $f$ represent frequency [Hz] and $G_0$ conductivity at frequency $f = 0$ [S].

## 2.7 Thermodynamic analysis

The theory in detail was referred to the previous literatures [Hitz *et al*., 2006, Almeida *et al*., 2009]. In short, the binding process was divided into the electrostatic and non-electrostatic interaction. The former and latter contribution was defined as $\Delta G_{el}$ and $\Delta G_{non\text{-}el}$, respectively. The total free energy was then $\Delta G = \Delta G_{el} + \Delta G_{non\text{-}el}$. The $\Delta G$ (= - $RT\ln K_{app,1}$) and $\Delta G_{non\text{-}el}$ (= - $RT\ln K_{app,2}$) values were obtained by an estimation of the apparent partitioning coefficient of HRP to vesicle $K_{app,1}$ defined in the complex formation model and $K_{app,2}$ in the distribution model, respectively. The important point is that the $\Delta G$ and $\Delta G_{non\text{-}el}$ values can be evaluated from the concentration dependency of the experimental data regarding the HRP-vesicle interaction.

## 2.8 Visualization of lysine residues on HRP

The information concerning the structure of HRP was acquired from Protein Data Base (PDB). Its ID was 1hch. The file of 1hch was recorded as 1hch.pdb to be restored in the software for visualization. The UCSF Chimera 1.14 (http://www.cgl.ucsf.edu/chimera/) that was free software was used.

## 3. Results and Discussion

### 3.1 Interaction between HRP and Lipid Planar membranes

The amount of HRP adsorbed on the lipid membrane was measured from the frequency change using QCM. The larger the frequency reduction width, the larger the amount of HRP adsorbed on the lipid membrane [Vu *et al*., 2009]. The experimental results showed that surfactants such as AOT adsorb more than phospholipids such as DOPC (**Figure 4-1 (a)**). Furthermore, it was shown that the amount of protein adsorbed to the vesicle membrane was larger than that of the planar lipid membrane in which the fluctuation of the whole membrane was suppressed regardless of the type of lipid (**Figure 4-1 (b)**). This suggests that the fluctuation of the whole membrane such as vesicles contributes to the adsorption rather than the effects of translational diffusion and vertical protrusion.
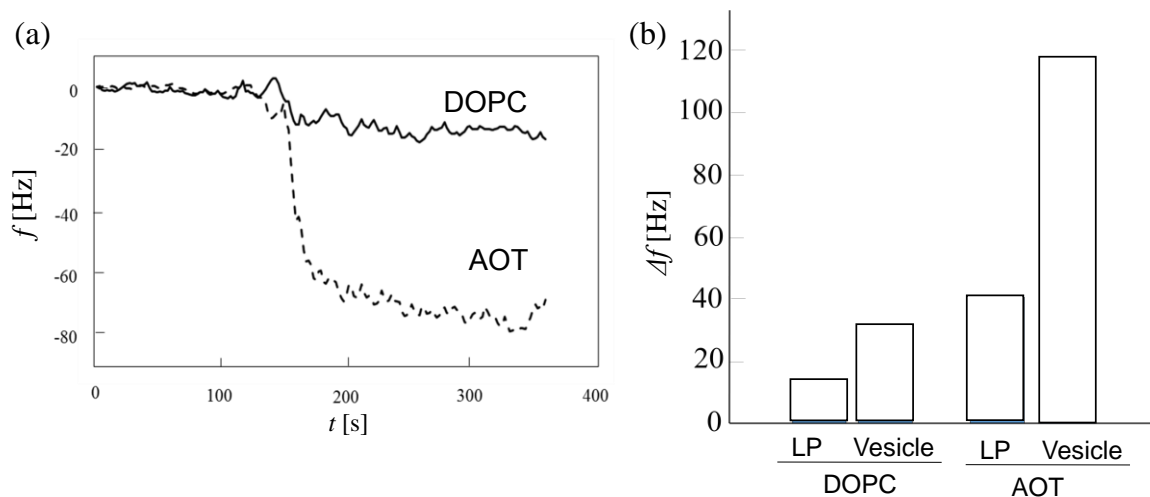


**Figure 4-1 Comparison of the amount of protein adsorbed on planar membrane and vesicle membrane** (a) Effect of HRP addition to frequency change of QCM (lipid planar membranes DOPC,AOT), (b) Amounts of HRP adsorbed to lipid planar membranes and vesicles.

## 3.2 Interaction between HRP and vesicles

The amount of protein adsorbed to vesicles can be measured by QCM combined with a immobilization technique of the lipid membrane. This system is a powerful tool for the measurement of the mass of adsorbed protein from the change in frequency of a crystal oscillator that vibrates at a fixed frequency (resonance frequency) [Vu *et al.*, 2009]. As shown in **Figure 4-2 (a)**, the frequency decrease occurred between 180 and 300 seconds ($f_{pro}$) corresponds to the mass of HRP adsorbed to vesicles. To compare the amount of adsorbed HRP to vesicles, the $f_{pro}$ value was normalized by the immobilized amount of lipid membranes on the QCM electrode ($f_{mem}$), which corresponds to the adsorbed mass of HRP per one vesicle. The obtained $f_{pro}$ / $f_{mem}$ values for individual vesicles are shown in **Figure 4-2 (b)**. The adsorbed amounts of HRP on the AOT and SDBS/DA vesicles were larger than on other phospholipid vesicles. This may be due to the negative charge of AOT and SDBS.
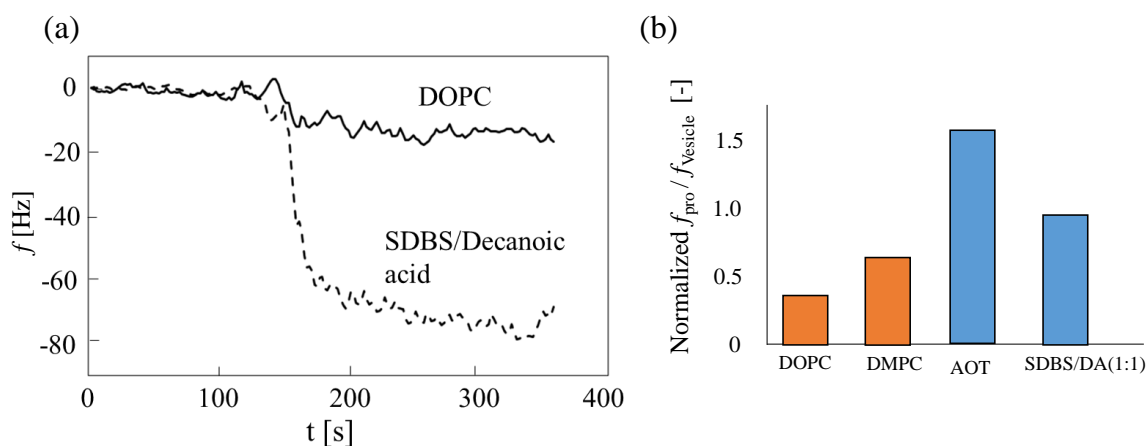


**Figure 4-2 Comparison of the effect of the amount of protein adsorbed on the vesicle membrane by the difference in the type of lipid constituting the vesicle**

(a) Effect of HRP addition to frequency change of QCM, (b) Amounts of HRP adsorbed to vesicles.

## 3.3 Thermodynamic analysis of HRP binding

The driving force for HRP-vesicle interaction investigated in the last section was then examined in the thermodynamic approach [Hitz *et al*., 2006, Almeida *et al*., 2009]. This thermodynamic approach requires the concentration dependency of HRP for the HRP-vesicle interaction like **Figures 4-2 (a) and (b)**. These experimental data were then analyzed according to the section 2.7 to obtain the electrostatic contribution $\Delta G_{el}$. The values of $\Delta G_{el}$ = -2.4 kJ/mol (25.0%) for DOPC and -3.2 kJ/mol (23.2%) for DMPC were obtained. On the other hand, SDBS/DA and AOT indicated the values of $\Delta G_{el}$ = -2.9 kJ/mol (31.1%) and -3.1 kJ/mol (29.0%), respectively. The values in parenthesis means the contribution of $\Delta G_{el}$ to the total free energy $\Delta G$. The electrostatic contribution to HRP-vesicle interaction was almost similar between zwitterionic phospholipid systems and negatively charged surfactant systems.

From these results, it was suggested that non-electrostatic interaction (approx. 70%) is the main driving force for the HRP-vesicle interactions.


## 3.4 Binding properties of HRP to lipid membranes

As shown in Chapter 2, the orientation of the protein relative to the lipid membrane can be discussed by measuring the $\pi$-$A$ isotherm. The $\pi$-$A$ isotherm is shifted to the higher $A$ value when the protein is inserted into the vesicle membrane. This is because the change in the occupied area of the lipid increases due to the protein insertion. In contrast, no significant shift of the isotherm results from either the peripheral binding of HRP or no interaction between HRP and lipid membranes. With the fact in mind, the impact of HRP addition to the $\pi$-$A$ isotherm is then shown in **Figure 4-3**. **Figure 4-3 (a)** shows no significant shift of the $\pi$-$A$ isotherm by the HRP

addition, possibly suggesting either the peripheral binding of HRP or no interaction between HRP and DOPC membranes. Considering also the amount of HRP adsorbed on DOPC vesicles (**Figure 4-2 (b)**), HRP was most likely to peripherally bind to DOPC membranes. The same was true for DMPC membranes. On the other hands, **Figure 4-3 (b)** obviously demonstrated the shift of $\pi$-*A* isotherm to the higher *A* value, strongly suggesting the insertion of HRP into SDBS/DA membranes. The same was true for AOT membranes (data not shown).

The dynamic property of the surface of lipid membranes is related to the rotational Brownian motion of headgroup of lipids. The dielectric dispersion analysis was then measured to estimate this mobility of headgroups [Shimanouchi *et al*., 2011]. **Figure 4-4 (a)** shows the typical dielectric spectra for DOPC. This included lateral diffusion of DOPC molecules, the rotational Brownian motion of its headgroup, and water molecule bound to DOPC. The characteristic frequency of the rotational Brownian motion $f_{c2}$ was 50 MHz corresponding to approx. 2.0 ns. Relaxation time for other lipids was shown in **Figure 4-4 (b)**. The order of relaxation time was DMPC > DOPC > SDBS/DA > AOT. Here, DOPC and DMPC bears phosphocholine group $PO_2^--N^+(CH_3)_3$ as headgroup. In contrast, AOT and SDBS bear the sulfonate group $SO_3^-Na^+$ as headgroup. The size of $SO_3^-Na^+$ is smaller than $PO_2^--N^+(CH_3)_3$. Then, the size effect of headgroup was likely to determine the interaction between headgrpups. Likewise, the acyl-acyl interaction would also affect the interaction between headgroups of lipids: *i.e.* branched C8 in AOT indicated the acyl-acyl interaction weaker than linear C14 in DMPC and linear C16 in DOPC (see **Scheme 4-1**). Therefore, the above order for relaxation time suggested that the interaction between headgroups for surfactant vesicles was weak as compared with that in phospholipid

vesicles.

From **Figures 4-3 and 4-4**, HRP could easily push aside AOT and SDBS due to the weak interaction between surfactants. This nature was likely to relate to the HRP insertion into the lipid membrane phase.
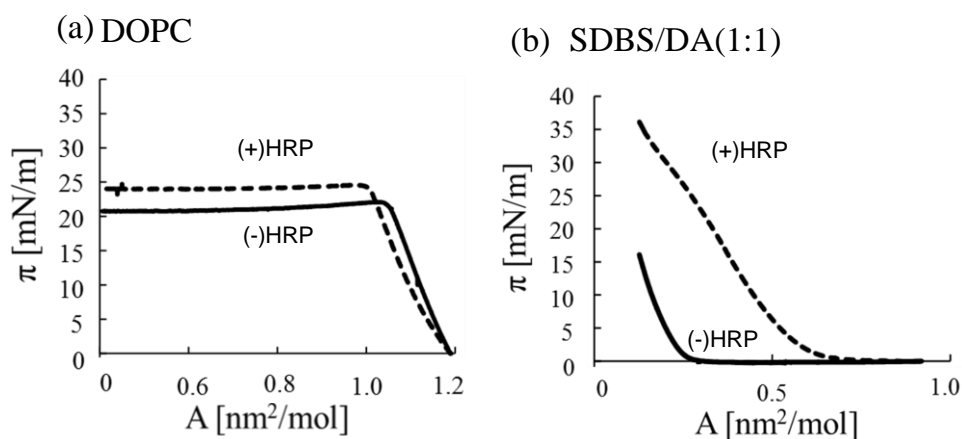


(a) DOPC    (b)  SDBS/DA(1:1)

**Figure 4-3 Effect of HRP addition to surface pressure isotherm** for (a) DOPC and (b) SDBS/DA monolayer membranes.
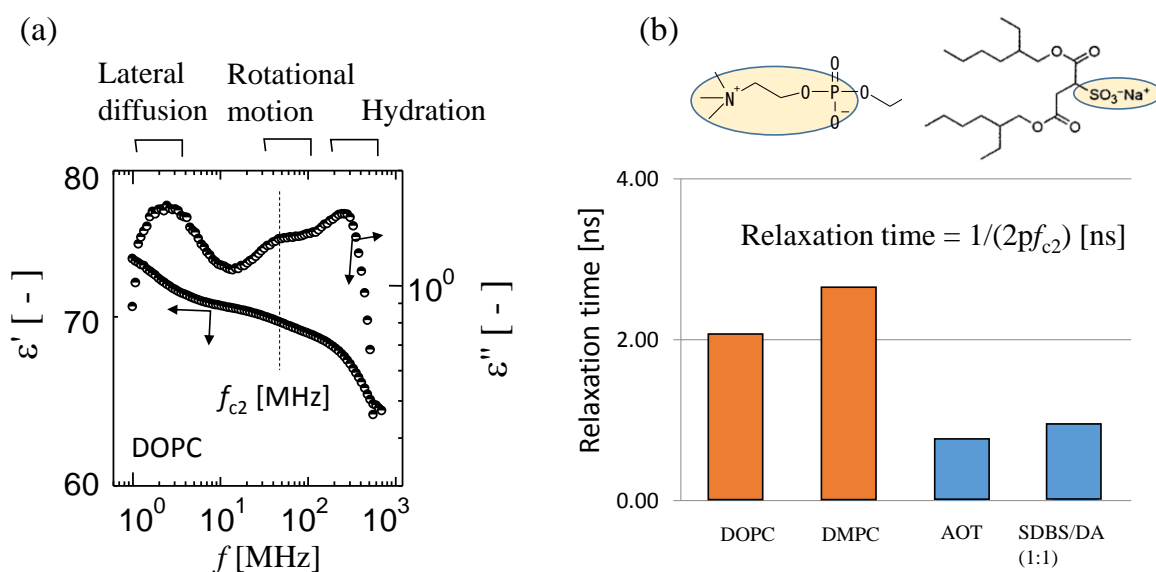


**Figure 4-4 Results of dielectric dispersion analysis.** (a) Typical dielectric spectra for DOPC. (b)The relaxation time at the rotational motion.

**3.5 Possible binding mechanisms**

Two scenarios to describe the partitioning behavior of proteins, including their insertion, are promising: a free volume [Kupiainen *et al*., 2005] and crevice/pothole [Shimanouchi *et al*., 2011]. A simulation study regarding the free volume in lipid membranes has predicted the presence of voids in the membrane interior and interface [Kupiainen *et al*., 2005]. Meanwhile, the formation probability of voids with more than 1 mm in size is quite low for HRP binding (its size is 2.4 nm in diameter [O'Brien *et al*., 2001]). Therefore, a discussion based on the free volume is not rational. A plausibility of crevice/pothole-based scenario will be discussed alternatively. The headgroup mobility at the surface of vesicle membranes generates the crevice/pothole, which is hydrophobic (low permittivity) environment [Shimanouchi *et al*., 2011]. Small-sized proteins bind to the crevice/pothole via electrostatic interaction in the first and the subsequent non-electrostatic interaction occurs at the low dielectric environment to reinforce the instable hydrogen bonds [Shimanouchi *et al*., 2014]. Whether the binding of protein to the vesicle membrane is also driven in a same manner as the case of small molecules is herein discussed.

The electrostatic interaction between both brings about prior to the non-electrostatic interaction depends on the net charge of HRP. The net charge of HRP is slightly positive under the present solution because the isoelectric point of HRP is pI = 7.2 [Fukuma *et al*., 2017] ~ 9 [Zakharova *et al*., 2011]. This is because of the presence of six lysines in the HRP molecule (Lys65, 84, 149, 174, 232, and 241 [Welinder 1979]). According to the literature [O'Brien *et al*., 2001], the reactivity of Lys to the chemical modification depends on its position: Lys232 is the most reactive; Lys241 and Lys174 are less reactive; Lys65, Lys84, and Lys149 are hardly modified.

The typical agents for chemical modifications of Lys are maleic anhydride derivatives or bis($N$-hydroxysuccinimidyl succinate) derivatives [Gajhede $et$ $al$., 1997] that are comparable to the size of $PO_2^--N^+(CH_3)_3$ and $SO_3^-Na^+$. It is therefore considered that HRP can interact with lipid membranes via electrostatic interaction between Lys232 (Lys241 and Lys174) and negative charge of headgroup in lipid molecules ($PO_2^--N^+(CH_3)_3$ or $SO_3^-Na^+$). Then, the location of Lys232, Lys241, and Lys174 were depicted by using the UCSF Chimera 1.14 in **Figure 4-5 (a)**. Six Lys residues were red-colored parts, indicating that Lys 174, Lys 232, and Lys 241 are located at the surface of HRP as compared with other Lys residues. Therefore, the electrostatic interaction between Lys 232 (Lys241 and Lys174) and negatively charged group of lipid molecules would be rational. Therefore, the interaction between HRP and vesicle membranes at the first step would be an electrostatic interaction rather than non-electrostatic interaction (**Figure 4-5 (b)**). This interpretation is in agreement with the previous study regarding the insertion of b-peptide to phospholipid vesicles [Hitz $et$ $al$., 2006].

Next, the possibility that HRP bound to the crevice/pothole on lipid membranes is discussed. The present experiment with respect to the HRP-vesicle interaction was not controversial to the small-sized proteins as reported previously [Shimanouchi $et$ $al$., 2014], which implied the binding of HRP to the crevice/pothole on lipid membranes. The crevice/pothole has been estimated to have the similar size to the hydrophobic fluorescence probe, sodium 8-anilino-1-naphthalenesulfonate (ANS: 0.93 nm in diamter) [Shimanouchi $et$ $al$., 2011]. Therefore, the size of HRP (2.4 nm in diameter [O'Brien $et$ $al$., 2001]) is presumably too large to use the crevice/pothole for the direct insertion of HRP. Besides, the conformation of HRP is considerably stable.

The reason is that the index for the intramolecular hydrogen bonding stability $\rho_{pr}$ was estimated to be 7.4±0.4, according to the literature [Shimanouchi *et al.*, 2013]. It is noted that the protein molecule with stable conformation indicates the high $\rho_{pr}$ value [Fernández *et al.*, 2003]. There is also a report that the binding of HRP into the vesicle membrane interior gave a small impact on the conformation neighboring the heme iron as the reaction center [Tang *et al.*, 2002]. These findings probably relate to four disulfide bonds formed in HRP molecule [Gajhede *et al.*, 1997]. Therefore, HRP bound to the crevice/pothole without a large conformational change.

Here, the possibility of HRP aggregation on vesicle membranes is addressed. Generally, the protein with low $\rho_{pr}$ value favors its association to form the dimer/ oligomer, aggregation, or fibrillation [Fernandez *et al.*, 2003]. As stated in the last paragraph, the conformation of HRP that is quite stable due to the high $\rho_{pr}$ value is stable over the binding to vesicle membranes. It is therefore considered that HRP interacted with vesicle membranes without any association or aggregation (**Figure 4-5 (b)**).

Finally, the insertion step of HRP is discussed. The electrostatic interaction between Lys in HRP and the headgroups is modulated by their mobility at the membrane surface. The weak interaction between headgroups like surfactants was most unlikely to act as the barrier to the HRP insertion (**Figure 4-3 (b)**). Furthermore, the interaction process coupled with non-electrostatic interactions as discussed in the section 3.3, which resulted in the stable insertion state of HRP into vesicle membranes. Inversely, the strong interaction between headgroups like phospholipids acted as the barrier to the HRP insertion. This nature would result in the peripheral binding of HRP to vesicle membranes. Besides, the long acyl chain of phospholipid could act as the

steric barrier to the insertion of HRP molecules, as compared with the short acyl chain like AOT.

From these discussion, HRP-vesicle interaction depicted in **Figure 4-5 (b)** appeared to be explained by a same scenario as the small-sized proteins as reported before [Shimanouchi *et al.*, 2014].
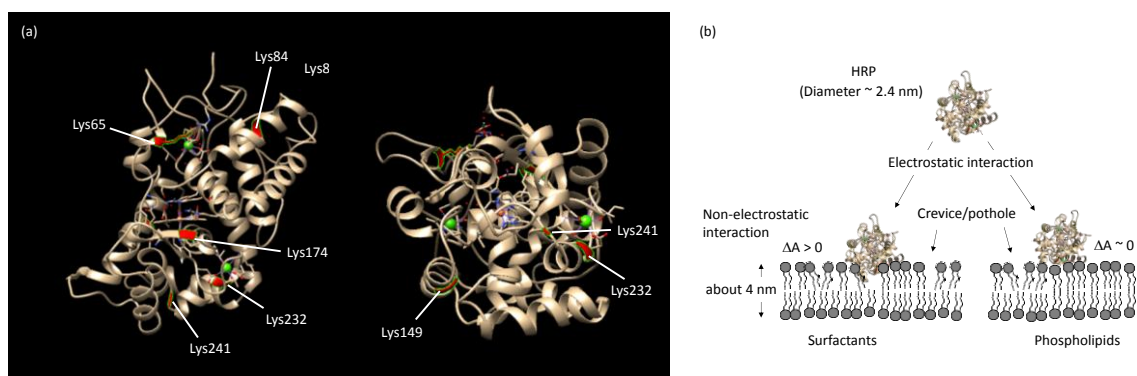


**Figure 4-5** (a) Topology of lysines on HRP (1hch.pdb). (b) Schematic illustration on HRP-vesicle interaction

## 4. Conclusion

HRP interacted with the vesicle membranes according to the consecutive process. First, HRP was likely to bind to the vesicle membrane based on the electrostatic interaction between accessible Lys on HRP and negatively charged parts of headgroups, followed by the insertion of HRP into membranes under the weak interaction between headgroups of lipids. This step was driven in a non-electrostatic manner. Otherwise, HRP was peripherally located at the membrane surface of vesicles. As a consequence, the weak interaction between headgroups of lipids enhanced the HRP-vesicle interaction based on HRP adsorption. The present finding would be helpful for a deeper understanding of the translocation or insertion of positively charged polypeptide (protein) to negatively charged phospholipid vesicles [Almeida *et al*., 2009] and heat-induced translocation of partially-denatured proteins [Umakoshi *et al*., 1998a, Umakoshi *et al*., 1998b].

# References

Almeida, P. F.; Pokorny, A., Mechanisms of Antimicrobial, Cytolytic, and Cell-Penetrating Peptides: From Kinetics to Thermodynamics. *Biochemistry*, **48**, 8083-8093 (2009)

Barauskas, J.; Johnsson, M.; Tiberg, F., Self-Assembled Lipid Superstructures: Beyond Vesicles and Liposomes. *Nano Lett.*, **5**, 1615-1619 (2005)

Bolinger, P.-Y.; Stamou, D.; Vogel, H., Integrated Nanoreactor Systems: Triggering the Release and Mixing of Compounds Inside Single Vesicles. *J. Am. Chem. Soc*., **126**, 8594-8595 (2004)

Elani, Y.; Law, R. V.; Ces, O., Vesicle-based artificial cells as chemical microreactors with spatially segregated reaction pathways. *Nature Comm*., **5**, Article number 5305 (2014)

Fernández, A.; Berry, R. S., Proteins with H-bond packing defects are highly interactive with lipid bilayers: Implications for amyloidogenesis. *Proc. Natl. Acad. Sci. U. S. A*., **100**, 2391-2396 (2003).

Gajhede, M.; Schuller, D. J.; Henriksen, A.; Smith, T.; Poulos, T. L., Crystal structure of horseradish peroxidase C at 2.15 A resolution. *Nat. Struct. Biol*., **4**, 1032-1038 (1997)

Hayashi, K.; Iwai, H.; Kamei, T.; Iwamoto, K.; Shimanouchi, T.; Fujita, S.; Nakamura, H.; Umakoshi, H., Tailor-made drug carrier: Comparison of formation-dependent physicochemical properties within self-assembled aggregates for an optimal drug carrier. *Colloids Surf. B*, **152**, 269-276 (2017)

Hitz, T.; Iten, R.; Gardiner, J.; Namoto, K.; Walde, P.; Seebach, D., Interaction of α-and β-Oligoarginine-Acids and Amides with Anionic Lipid Vesicles: A Mechanistic

and Thermodynamic Study. *Biocheistry*, **45**, 5817-5829 (2006)

Jesorka, A.; Orwar, O., Liposomes: technologies and analytical applications. *Ann. Rev. Anal. Chem.*, **1**, 801-832 (2008)

Kuboi, R.; Shimanouchi, T.; Yoshimoto, M.; Umakoshi, H., Detection of Protein Conformation under Stress Conditions Using Liposomes As Sensor Materials. *Sensors and Materials*, **16**, 241-254 (2004)

Kupiainen, M.; Falck, E.; Ollila, S.; Niemelä, P.; Gurtovenko, A. A.; Hyvönen, M. T.; Patra, M.; Karttunen, M.; Vattulainen, I., Free volume properties of sphingomyelin, DMPC, DPPC, and PLPC bilayers. *J. Comp. Theor. Nanosci.*, **2**, 401-413 (2005)

Nomura, S. M.; Tsumoto, K.; Hamada, T.; Akiyoshi, K.; Nakatani, Y.; Yoshikawa, K.; Gene Expression within Cell‐Sized Lipid Vesicles. *ChemBioChem*, **4**, 1172-1175 (2003).

O'Brien, A. M.; O'Fagain, C.; Nielsen, P. F.; Welinder, K. G., Location of Crosslinks in chemically stabilised Horseradish Peroxidase. Implications for design of crosslinks. *Biotechnol. Bioeng.*, **76**, 277-284 (2001)

Ryan, B. J.; Carolan, N.; O'Fagain, C., Horseradish and soybean peroxidases: comparable tools for alternative niches? *Trends Biotechnol.*, **24**, 355-363 (2006)

Shimanouchi, T.; Ishii, H.; Yoshimoto, N.; Umakoshi, H.; Kuboi, R., Calcein permeation across phosphatidylcholine bilayer membrane: Effects of membrane fluidity, liposome size, and immobilization. *Coll. Surf. B*, **73**, 156-160 (2009)

Shimanouchi, T.; Sasaki, M.; Hiroiwa, A.; Yoshimoto, N.; Miyagawa, K.; Umakoshi, H.; Kuboi, R., Relationship between the mobility of phosphocholine headgroups of liposomes and the hydrophobicity at the membrane interface: A characterization with spectrophotometric measurements. *Coll. Surf. B*, **88**, 221-230 (2011)

Shimanouchi, T.; Nishiyama, K.; Hiroiwa, A.; Vu, H. T.; Kitaura, N.; Umakoshi, H.; Kuboi, R., Growth Behavior of A β Protofibrils on Liposome Membranes and Their Membrane Perturbation Effect. *Biochem. Eng. J.*, **71**, 81-88 (2013).

Shimanouchi, T.; Yoshimoto, N.; Hiroiwa, A.; Nishiyama, K; Hayashi, K.; Umakoshi, H.; Relationship between the mobility of phosphocholine headgroup and the protein–liposome interaction: A dielectric spectroscopic study. *Coll. Surf. B*, **116**, 343-350 (2014)

Tang, J.; Jiang, J.; Song, Y.; Peng, Z.; Wu, Z.; Dong, S.; Wang, E., Conformation change of horseradish peroxidase in lipid membrane. *Chem. Phys. Lipids*, **120**, 119-129 (2002)

Umakoshi, H.; Yoshimoto, M.; Shimanouchi, T.; Kuboi, R.; Komasawa, I., Model System for Heat‐Induced Translocation of Cytoplasmic β‐Galactosidase across Phospholipid Bilayer Membrane. *Biotech. Prog.*, **14**, 218-226 (1998a)

Umakoshi, H.; Shimanouchi, T.; Kuboi, R., Selective separation process of proteins based on the heat stress-induced translocation across phospholipid membranes. *J. Chromatogr. B*, **711**, 111-116 (1998b)

Umakoshi, H.; Suga, K.; Use Liposome as a Designable Platform for Molecular Recognition ~ from "Statistical Separation" to "Recognitive Separation"~. *Solvent Extr. Res. Dev., Jpn.*, **20**, 1-13 (2013)

Veitch, N. C., Horseradish peroxidase: a modern view of a classic enzyme. *Phytochemnstry*, **65**, 249-259 (2004)

Vu, H. T.; Shimanouchi, T.; Ishii, H.; Umakoshi, H.; Kuboi, R., Immobilization of intact liposomes on solid surfaces: A quartz crystal microbalance study. *J. Colloid Interface Sci.*, **336**, 902-907 (2009)

Welinder, K. G., Amino Acid Sequence Studies of Horseradish Peroxidase. *Eur. J. Biochem.*, **96**, 483-502 (1979)

Wimley, W. C.; White, S. H., Experimentally determined hydrophobicity scale for proteins at membrane interfaces. *Nat. Struct. Biol.*, **3**, 842-848 (1996)

Zakharova, G. S.; Uporov, I. V.; Tishkov, V. I., Horseradish peroxidase: Modulation of properties by chemical modification of protein and heme. *Biochemistry (Moscow)*, **76**, 1391-1401 (2011)

Zhang, Z.; Shogawa, M.; Yamashita, K.; Noda, M., Real-time characterization of fibrillization process of amyloid-beta on phospholipid membrane using a new label-free detection technique based on a cantilever-based liposome biosensor. *Sens.Act. B*, **236**, 893-899 (2016).

# Chapter 5

# Application to high sensitive and selective detection system

## 1. Introduction

Many kinds of capsules for encapsulating drugs in DDS have been widely studied. Also, biosensors for detecting proteins have been studied. There are various materials as detection units in biosensors. One of promising materials is vesicles [Kaneda *et al*., 2000, Walde *et al*., 2014, Erb *et al*., 2000, Olea *et al*., 2008]. Vesicles are closed vesicles composed of lipid bilayer membranes. In DDS, a controlled release of reagents encapsulated in vesicles is expected [Cabane *et al*., 2011]. Vesicles have the permeability barrier to cations and anions [Bangham *et al*., 1965, Shi *et al*., 2002]. The permeability responds to the outer environmental conditions. Besides, vesicles have the biocompatibility due to the similar membrane structure to biological membranes.

The relationship between protein-vesicle interaction kinetically elevated the membrane permeability [Kuboi *et al*., 2004]. The characteristics of proteins including secondary structure was likely to give the different leakage behavior of calcein [Kuboi *et al*., 2004]. However, the leakage mechanism of calcein induced by the protein was still unclear. Even in the case of calcein leakage using ultrasound, it was not clarified whether pierce a hole or open on the liposomal membranes [Ahmed *et al*., 2016]. If the mechanism of protein-enhanced permeability can be elucidated, it will lead to a development of detection units for biosensors and of high-performed material for DDS.

In Chapter 4, the author has clarified that HRP-vesicle interaction was driven by the consecutive process: the first process based on the electrostatic interaction and the subsequent process based on non electrostatic interaction. In the first process,

positively charged lysine residues on horse radish peroxidase (HRP) was found to bind to the negatively charged group in headgroup of surfactants or phospholipids at the membrane interface of vesicles. In the of weak interaction between headgroups of lipids (vesicles were instable), HRP was inserted into the interior of vesicle membranes via non-electrostatic interaction. This interaction induced the strong leakage of calcein. On the other hand, HRP peripherally bound to the membrane surface if the interaction between headgroups of lipids were strong, which resulted in low leakage of calcein. Thus, the insertion behavior of HRP into vesicle membranes due to the electrostatic and non-electrostatic interaction determined the calcein leakage. This mechanism might be applicable to other proteins. If so, vesicle might be able to detect the proteins with high sensitivity.

Based on these backgrounds, in Chapter 5, the author considered that the increase in membrane permeability by proteins other than HRP is also affected by the protein-vesicle interaction. Such interactions between proteins and vesicles were analyzed by utilizing the compression properties of lipids [Phillips *et al*., 1968, Yun *et al*., 2003], and comparing with leakage rate of encapsulated fluorescent agents. The mechanism of membrane permeability increase by protein was finally discussed.

## 2. Materials and Methods

### 2.1 Materials

The lipids and reagents used were 1,2-dioleoyl-sn-glycero-3-phosphocholine (DOPC), 1-palmitoyl-2-oleoyl-sn-glycero-3-phosphocholine (POPC), sorbitan monolaurate (Span20), polyoxyethylene sorbitan monolaurate (Tween20), sorbitan monopalmitate (Span40), polyoxyethylene sorbitan monopalmitate (Tween40), sorbitan monooleate (Span80), polyoxyethylene sorbitan monostearate (Tween60), decanoic acid (DA), peroxidase from horseradish (HRP), and lysozyme from Egg White (Lys) were purchased from Wako Pure Chemicals Ltd (Osaka, Japan). 1,2-dipalmitoyl-sn-glycero-3-phosphocholine (DPPC), 1,2-dimirystoyl-sn-glycero-3-phosphocholine (DMPC), sodium dodecylbenzene sulfonate (SDBS), and sodium di-2-ethylhexylsulfosuccinate (AOT) were purchased from Tokyo Chemical Industry Co., Ltd. (Tokyo, Japan). 2-dioleoyl-sn-glycero-3-[phosphor-rac-(3-lysyl(1-glycerol))] (DOPG), sepharose 4B, and Triton X-100 were purchased from Sigma-Aldrich Japan (Tokyo, Japan). Amyloid β protein with 40 amino acid residues (Aβ) was purchased from PEPTIDE INSTITUTE, INC. (Osaka, Japan). Calcein was purchased from Dojindo (Kumamoto, Japan).

### 2.2 Vesicle Preparation

Vesicles were prepared according to the previous method [MacDonald *et al*., 1991, Manosroi *et al*., 2003, Guo *et al*., 2009 ]. Phospholipids and Surfactants were dissolved in a chloroform solution (10 mg/mL). The organic solvent was removed by evaporation in a rotary evaporator. The residual lipid film, after drying under a vacuum overnight, was hydrated with the 100 mM calcein solution to form multilamellar

liposomes (MLVs). For the preparation of unilamellar vesicles by extrusion, the MLV suspension was subjected to five cycles of freezing and thawing, and passed 15-times through two stacked polycarbonate filters with 100 nm pores (Nuclepore, Costar, Cambridge,MA) at room temperature by using an extrusion device (Liposofast; Avestin Inc.). To prepare vesicles entrapping calcein, free calcein was removed by a gel permeation chromatography (Sepharise 4B, φ 15mm, height 150 mm). The vesicles which was used in Chapter5 were listed in **Table 5-1**.

**Table 5-1 Entry number of lipids for vesicles**

| Entry | Lipid | Charge | Phase at 25°C |
|:---:|:---:|:---:|:---:|
| 1 | DOPC | Zwitterionic | L |
| 2 | DPPC | Zwitterionic | G |
| 3 | DMPC | Zwitterionic | G |
| 4 | POPC | Zwitterionic | L |
| 5 | DOPG | Negative | G |
| 6 | DOPC/DPPC (50:50) | Zwitterionic | $l_d + l_o$ |
| 7 | Span20/Tween20 (75:25) | Zwitterionic | - |
| 8 | Span40/Tween40 (75:25) | Zwitterionic | - |
| 9 | Span80/Tween60 (75:25) | Zwitterionic | - |
| 10 | SDBS/DA (50:50) | Negative | - |
| 11 | SDBS/DA (75:25) | Negative | - |
| 12 | AOT | Negative | - |

L: liquid-crystalline phase, G: Gel phase, $l_d$: liquid-disordered phase, $l_o$: liquid-ordered phase

## 2.3 Calcein leakage assay

A calcein leakage experiment was performed according to the previous literatures [Kuboi *et al*., 2004, Shimanouchi *et al*., 2009]. The vesicles entrapped calcein were prepared with a hydration method. In short, a lipid film was hydrated with calcein solution (100 mM). Size exclusion chromatography was performed to remove calcein not entrapped. The vesicles entrapped calcein (250 μM) and proteins (10 μM) were mixed, and the fluorescence intensity was measured at an excitation wavelength of 490 nm and a emission wavelength of 520 nm with a fluorescence spectrophotometer (FP6500). Finally, Triton-X 100 was added to disrupt the vesicles, and the maximum fluorescence intensity was measured to obtain the calcein leak rate *RF* value.

$$RF = 100 \times (I(t)\text{-}I_0)/(I_{\text{total}}\text{-}I_0) \ (\%) \qquad \textbf{(5-1)}$$

where $I(t)$ is the intensity at time $t$, and $I_0$ and $I_{\text{total}}$ are the intensities immediately after the start of the release analysis and immediately after the addition of Triton X-100, respectively. First-order kinetics were employed to analyze calcein release:

$$RF(t) = RF_{\text{max}}(1\text{-}\exp(\text{-}kt)) \qquad \textbf{(5-2)}$$

where $RF_{\text{max}}$ and $k$ represent the maximum value of *RF* and the release rate constant, respectively. To determine $RF_{\text{max}}$, all experiments were run until the value of calcein fluorescence reached a constant value.

## 2.4 Surface pressure analysis

Surface pressure analysis was performed to determine the $\pi$-A isotherm, and protein orientation analysis was performed by Small LB film making device FSD-220C (U.S.I Corp.) and LB LIFT CONTROLLER FSD-23(U.S.I Corp.) according to the previous report [Phillips and Chap Man 1968] . First, 60 μL of lipid (1 mM) dissolved in chloroform was dispersed in a water tank filled with ultrapure water. After allowing the lipid to stand at the gas-liquid interface for 15 minutes, pressure was applied to the surface with a barrier to investigate the change in occupied area (*A*) due to the change in the surface pressure ($\pi$). Lipid was dispersed and allowed to stand for 15 min, then 60 μL of protein solution (HRP: 5 mg / mL, Lys: 1.75 mg / mL, Aβ: 100 mM listed in **Table 5-2**) was added to the water bath, after 5 min left, Similarly, changes in *A* due to changes in $\pi$ were investigated, and the orientation pattern of proteins was discussed from the curve change due to the presence or absence of protein.

**Table 5-2. Molecular weight and isoelectric point of protein**

| Protein | Molecular weight [kDa] | pI |
|---------|------------------------|-----|
| HRP     | 40.2                   | 7.2 |
| Lys     | 14.3                   | 11  |
| Aβ      | 4.3                    | 5.2 |

# 3. Results and Discussion

## 3.1 Evaluation of leakage rate for various vesicles

In the first series of experiments, the calcein leakage behavior associated with the addition of proteins was monitored by using three types of vesicles since the lipid composition is the major factor for the calcein leakage [Shimanouchi *et al*., 2009]. The time-course of calcein leakage induced by HRP depended on the lipid composition of the vesicle, as shown in **Figure 5-1 (a)**. Specifically, a drastic leakage of calcein was detected in AOT-vesicles (entry 12) as compared with those for vesicles composed of DOPC (entry 1) and Span20/Tween20 (75:25) (entry 7). The calcein leakage is generally explained by the first-order kinetics [Shimanouchi *et al*., 2009, Sato *et al*., 1991] and the maximum release fraction ($RF_{max}$) and leakage rate constant ($k$) are the characteristic parameters for the calcein leakage behavior. Using **equation (5-2)**, both $RF_{max}$ and $k$ was estimated from the time-course of $RF$ value. For some cases, the $RF$ value reached plateau value by 1 hours and was used as $RF_{max}$. **Figure 5-1 (b)** shows the result of $RF_{max}$ and $k$ in all the vesicles tested herein. Both $RF_{max}$ and $k$ values for vesicles composed of detergents (entries 10-12) were relatively higher than those for vesicles composed of phospholipids (entries 1-6) and Span/Tween system (entries 7-9). Meanwhile, no definite influence of phase state on both $RF_{max}$ and $k$ for HRP-induced leakage of calcein was observed although the permeability to calcein depended on the phase state [Shimanouchi *et al*., 2009].
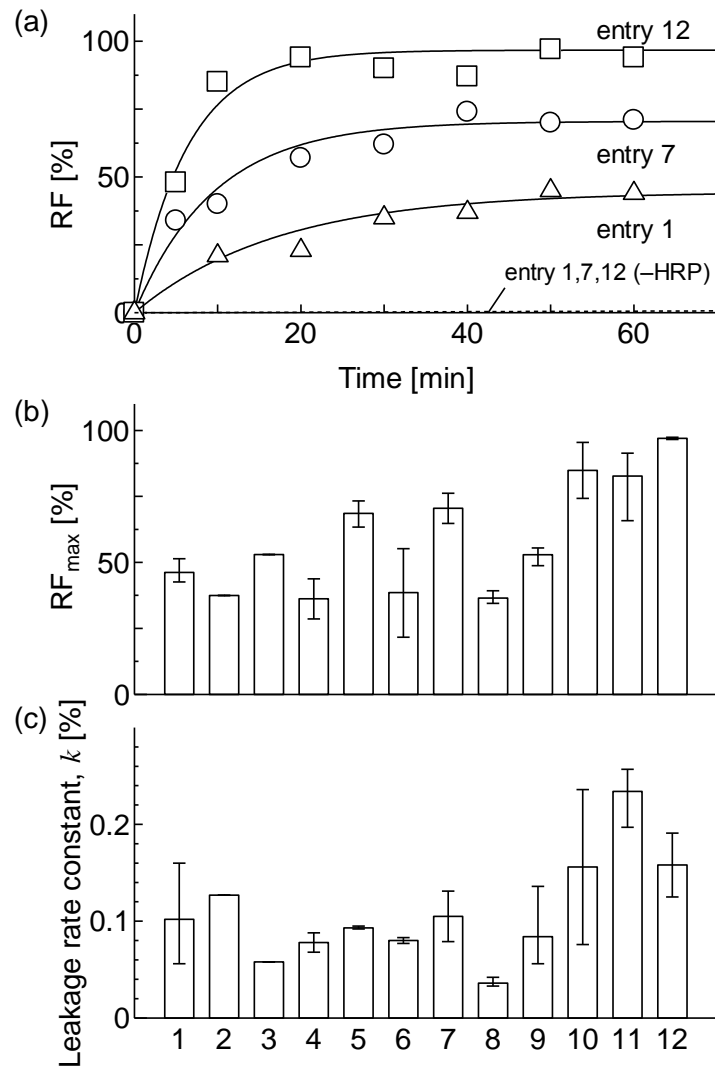
**Figure 5-1 Results of calcein leakage in various vesicles.** (a) Time-dependence of calcein leakage ($RF$) from various vesicles in the presence of HRP at room temperature. $R^2 = 0.970$, $0.984$, and $0.970$ for vesicles (entries 1, 7 and 12). Dotted curves represent the calcein leakage from vesicles (entries 1, 7, 12) without proteins. (b) Maximum of calcein leakage ($RF_{max}$) and (c) leakage rate constant ($k$) of various vesicles.

## 3.2 Effect of protein properties on leakage rate

The kinds of proteins is also the factor for calcein leakage [Kuboi *et al*., 2004]. In order to study the relationship between proteins and membranes more deeply, similar experiments were then carried out using Lys and Aβ that possess the different molecular weight and charge from HRP (**Table 5-2**). **Figure 5-2 (a)** shows the calcein leakage from DMPC vesicle (entry 3). Every proteins induced the calcein leakage behavior like a first-order kinetics. The $RF_{max}$ value was obtained in order of HRP > Lys > Aβ. The $k$ values for three proteins were almost same. The relatively small dependence observed in $RF_{max}$ and $k$ values was likely to be the small interaction between vesicles and proteins.
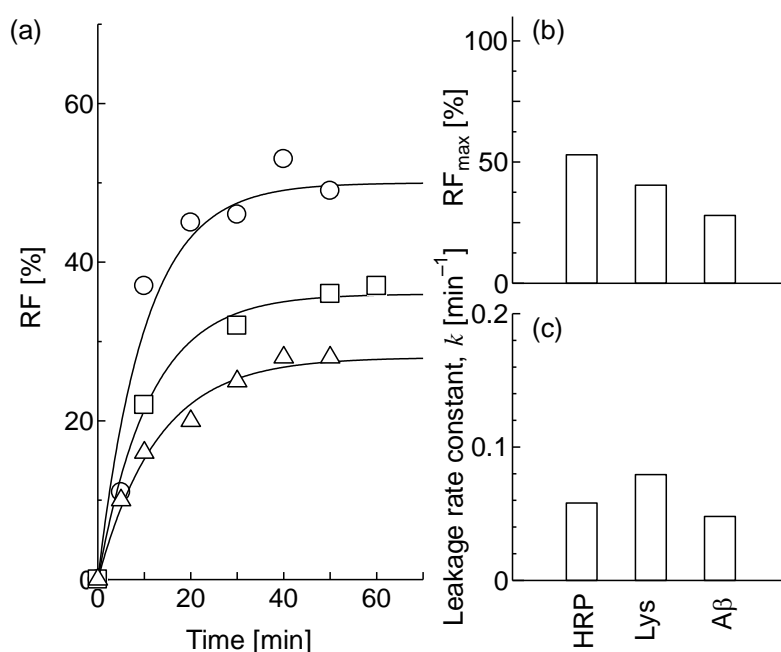


**Figure 5-2 Results of calcein leakage for various proteins in the same vesicle**

(a) Time-dependence of calcein leakage (*RF*) from DMPC vesicles (entry 3) in the presence of various proteins at room temperature. $R^2$ = 0.986, 0.991 and 0.992 for HRP (circle), Lys (square) and Aβ (triangle), respectively. (b) Maximum of calcein leakage ($RF_{max}$). (c) coefficient of leak rate ($k$) from DMPC liposomes in the presence of various proteins at room temperature.

The electrostatic interaction between proteins and vesicles easily contributes to the enhanced leakage of calcein. The effect of Lys with positively charge (pI ~ 11) on $RF_{max}$ and $k$ values was then examined. The trends in $RF_{max}$ and k for Lys was similar to HRP. Although the strong electrostatic attractive force between positively charged Lys and negatively charged vesicles (entries 10-12) was expected, the obviously elevated $k$ values was not confirmed as compared with that in the case of HRP (**Figures 5-3 (a) and (b)**).
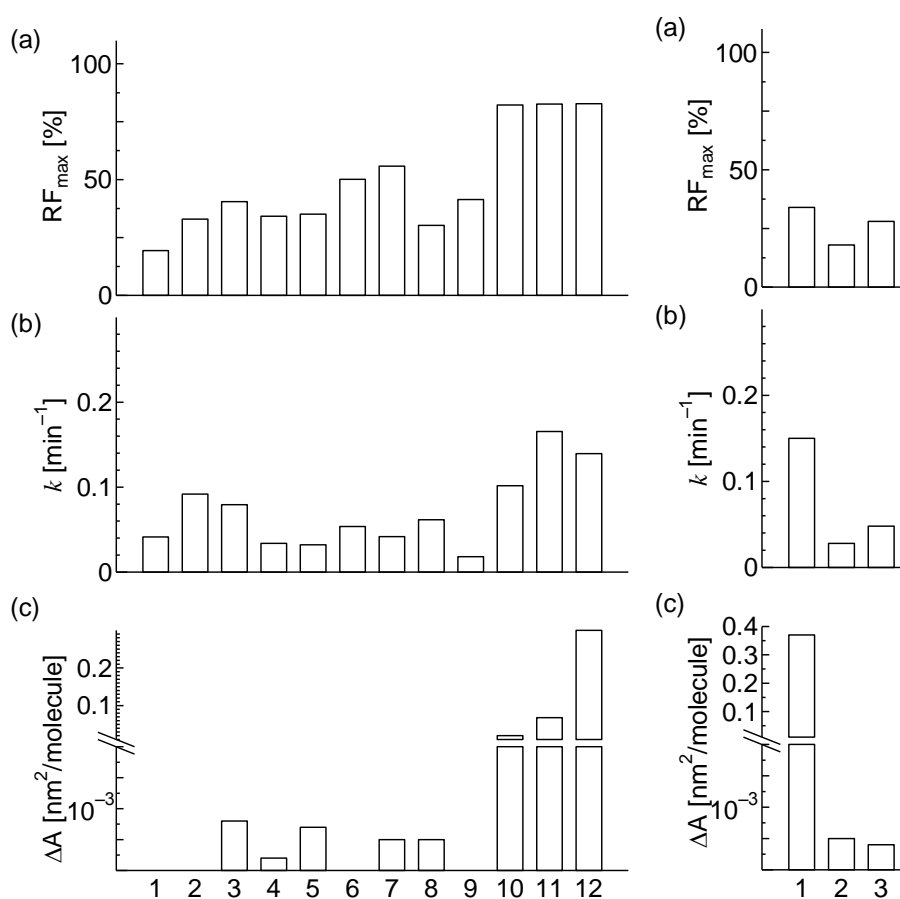


**(Left) Figure 5-3** (a) Maximum of calcein leakage ($RF_{max}$) and (b) leakage rate constant ($k$) of various vesicles. (c) Effect of Lys on ΔA value. **(Right) Figure 5-4** The case for Aβ.

**3.3 Relationship between protein orientation area and calcein leakage rate**

The size of molecular size of proteins is also the factor to determining the calcein leakage from the previous literature [Kuboi *et al.*, 2004]. The effect of molecular size of proteins including Aβ was therefore examined. From **Table 5-2**, the molecular weight of proteins used herein ranged from 4.3 − 14.3 kDa. Aβ also induced the calcein leakage and both the $RF_{max}$ and $k$ values for DOPC vesicles (entry 1) was significantly larger than those for other vesicles (entries 2 and 3) (**Figures 5-4 (a) and (b)**). In addition, the leakage behavior of DOPC vesicles (entry 1) induced by Aβ was comparable with those for vesicles (entries 10-12) by HRP and Lys, strongly suggesting that the size of proteins was not a major factor for the leakage mechanism of calcein.

Experiments were conducted using π-*A* isotherms which can compare the protein-vesicle interaction. The surface pressure isotherms of lipid membrane with and without proteins were compared as shown in **Figure 5-5 (a)**. A shift of isotherm to the higher *A* value range suggests that the protein molecules are oriented inside the lipid membrane [Wang *et al.*, 2015]. Accordingly, the orientation pattern of protein to lipid membranes could be divided into two groups: Group I that shifts to the higher *A* value range as in **Figure 5-5 (a)** and Group II with no significant shift as in **Figure 5-5 (b)**. To quantitatively discuss the interaction between HRP and lipid membranes, the shift of occupied area $\Delta A = A(+) - A(-)$ was defined where $A(+)$ and $A(-)$ are the occupied area at the drastic increase of π with and without proteins, respectively. The arrows in **Figures 5-5 (a) and (b)** are the indications for $A(+)$ and $A(-)$. **Figure 5-5 (c)** shows the $\Delta A$ values for each lipid membrane. Phospholipids (entries 1-6) and Span/Tween systems (entries 7-9) showed the low $\Delta A$ value and allotted into Group II. In contrast, the detergent systems (entries 10-12) showed the high $\Delta A$ value, corresponding to

Group I. Under our experimental condition, proteins might contribute to the area change of outer leaflet of vesicle membranes. Therefore, we discussed the relationship of this effect with the kinetics of calcein leakage in the following section.
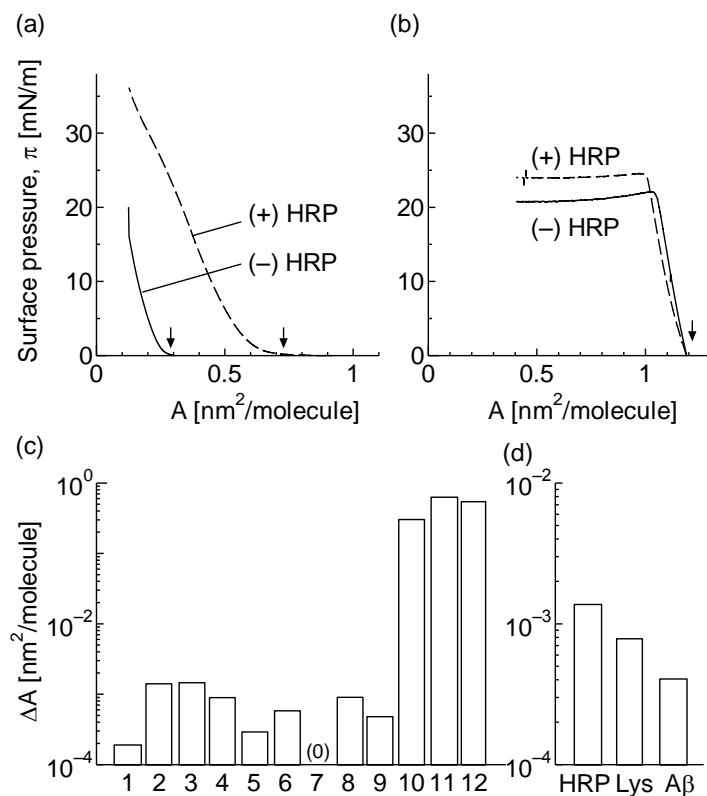


**Figure 5-5 π-A isotherms** of (a) AOT and (b) DOPC membranes with and without HRP. Arrows show the area with and without HRP. (c) Effect of HRP on $\Delta A$ of various membranes. (d) Effect of proteins on $\Delta A$ of DMPC membranes.

**Figure 5-6 (a)** shows the relationship between $\Delta A$ and $RF_{max}$ for twelve kinds of vesicles and three kinds of proteins. The $RF_{max}$ value positively correlated with $\Delta A$ value nevertheless to the lipids and proteins, although data were scattered. The same was true for the $k$ value (**Figure 5-6 (b)**). In actual, the leakage property not only depended on size of proteins but also the net charge of both proteins and lipids (see **Tables 5-1 and 5-2**). The linear correlation of $\Delta A$ with both $RF_{max}$ and $k$ values strongly suggested that the proteins interacted with vesicle membranes and perturbed the neighboring site around protein molecules. This implies that the perturbed area played a role for the leakage sites. The mechanism suggested herein is in agreement with the findings that denatured proteins [Kuboi *et al*., 2004] and cell penetrating peptides [Wang *et al*., 2015] gave the membrane perturbation. Hitz *et al.* have reported that the electrostatic interaction between positively charged peptides and negatively charged vesicles contributed to the calcein leakage by at most 30% and that the remaining contribution (~70%) is non-electrostatic interaction [Hitz *et al*., 2006]. The above peptides interacted with vesicles in an electrostatic manner at the first, followed by the hydrophobic interaction [Hitz *et al*., 2006]. Also, the dielectric study revealed that proteins could reduce the headgroup mobility of lipids within the membranes of vesicles, in the case using eight kinds of proteins and more than 20 kinds of zwitterionic vesicles [Shimanouchi *et al*., 2009]. Therefore, we considered that the proteins might interact with headgroups of the membranes of vesicles in an electrostatic manner, followed by the hydrophobic interaction. If the hydrophobic interaction between both was strong, protein molecule would penetrate into the vesicle membranes. That was probably why the calcein leakage was considered to be induced by the proteins.

The addition of HRP induced the morphological change of vesicles as shown in **Figures 5-6 (c)-(e)**. In the low $\Delta A$ value range (Group II), no definite morphological change was observed (similar to the vesicle alone (**Figure 5-6 (c)**). In the higher $\Delta A$ value range (Group I), some portion of spherical SDBS/DA vesicles easily changed its shapes into prolate or oblate (**Figure 5-6 (d)**). This morphological change associated with the increase in $\Delta A$ was reasonable in terms of the excess area of outer leaflet of vesicle membranes due to their penetration of proteins, according to the bilayer coupling model [Käs *et al*., 1991]. Besides, some portion of vesicles had the morphological change into the erythrocytes or stomatocytes in the case of SDBS/DA (entries 10 and 11) and AOT (entry 12) as shown in **Figure 5-6 (e)**, which was consistent with the previous report [Guo *et al*., 2009]. Such a dynamic change of vesicles was also likely to contribute to the drastic leakage of calcein.
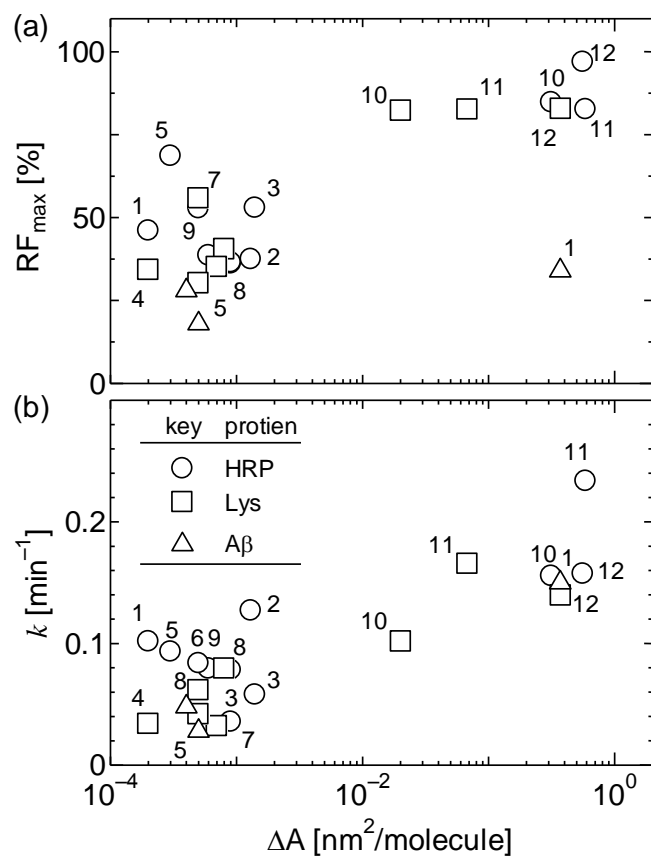
**Figure 5-6 Relationship between the protein-induced calcein leakage parameters**

(a) $RF_{max}$-$\Delta A$ and (b) $k$-$\Delta A$. Vesicle morphology in the absence and presence of proteins.

(c) DOPC alone (entry 1), (d) SDBS/DA (50:50) (entry 10) in the presence of HRP, and

(e) AOT (entry 12) in the presence of HRP.

## 3.4 Evaluation of detection limit concentration of various vesicles

The detection limit concentration was determined as an index for functional evaluation when using a vesicle as a sensor. It is suggested that the smaller the detection limit concentration, the higher the sensitivity of the sensor element. $RF_{max}$ at each concentration was determined by changing the concentration of the protein added in the calcein leakage experiment, and the detection limit concentration $C_{limit}$ was calculated for various vesicle membrane compositions from the value. The concentration at which $RF_{max}$ in the graph became 0 was calculated as the detection limit concentration. As a result, a tendency was found that the concentration of detection sensitivity was lower in surfactant vesicles than in phospholipid vesicles (**Figure 5-7**). It has been found that surfactant vesicles have a large increase in area due to the orientation of proteins to lipid membranes. From these results, it was suggested that the detection sensitivity could be increased in a membrane in which the vesicle membrane fluctuation was large and the protein was more easily oriented.

(a) DOPC

$C_{limit} =$ 0.60 [μM]

(b) SDBS/DA(1:1)

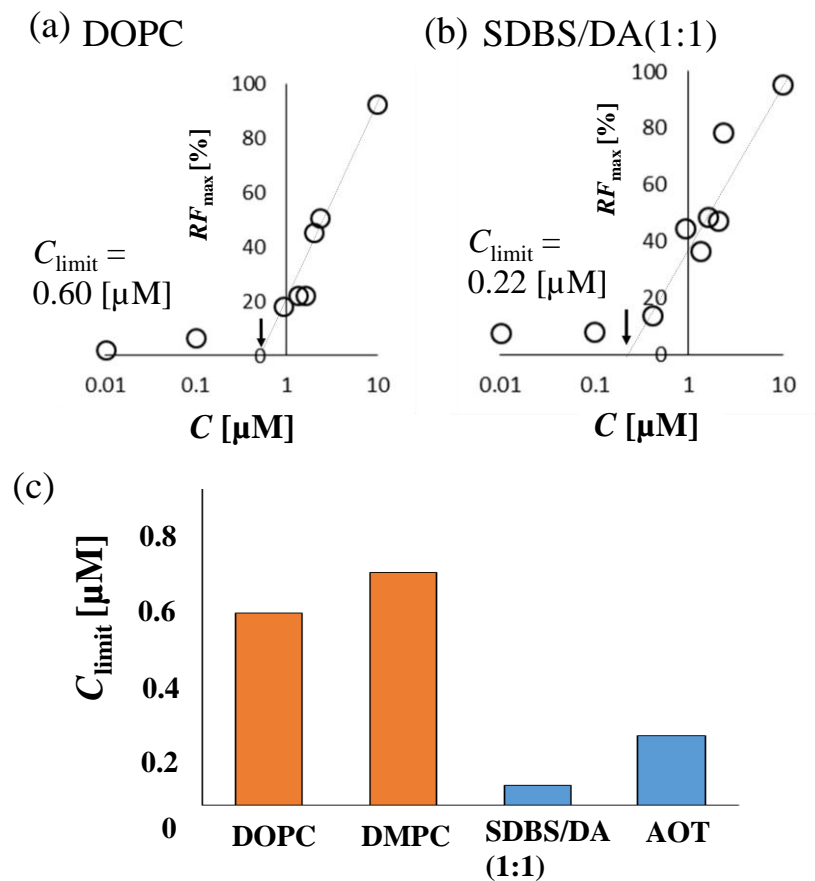$C_{limit} =$ 0.22 [μM]

(c)

**Figure 5-7 Evaluation of detection limit concentration of various vesicles based on correlation between protein(HRP) addition concentration and detection limit concentration** (a)In case of DOPC vesicle   (b)In case of SDBS/Decanoic acid (1:1) vesicle   (c)Comparison of detection limit concentration of phospholipid vesicle and surfactant vesicle

## 4. Conclusion

In conclusion, regardless of both the lipid composition of the membrane and the type of protein with different molecular weight or charge, it was found that the $RF$ tends to increase as $\Delta A$ increases. This suggests that proteins penetrated in the membrane have a sufficient effect on calcein leakage. The strong penetration of protein into vesicle membrane resulted in the morphological change of vesicles from spherical vesicles to erythrocyte or stomatocyte ones. Such dynamical change of vesicle membranes might contribute to the significant leakage of calcein. Previously it has been claimed that the hydrophobic interaction between protein and lipid membrane triggered the calcein leakage [Kuboi *et al*., 2004]. The strength of hydrophobic protein-vesicle interaction would relate to the penetration of protein. Thus, it can be useful knowledge for DDS and developing biosensor using proteins. It is noted that these results were the first time to in the field regarding the protein-induced calcein leakage behavior using the vesicles composed of Span and Tween (which are being studied for DDS in recent years) [Shi *et al*., 2002, Omokawa *et al*., 2010, Hayashi *et al*., 2011], which is beneficial to the DDS field.

From the viewpoint of comparison of detection limit concentration, it was suggested that surfactant vesicles could be a useful material in the future. Actually, when applied as a functional material, it is necessary to further improve the detection sensitivity (10 times or more) and selectivity (to serum protein) of the target protein by using a membrane fluctuation resistant vesicle.

# References

Ahmed, S. E.; Moussa, H. G.; Martins, A. M.; Al-Sayah, M. H.; Husseini, G. A., Effect of pH, ultrasound frequency and power density on the release of calcein from stealth liposomes. *Eur. J. Nanomed.*, **8**, 31 (2016)

Bangham, A. D.; Standish, M. M.; Watkins, J. C., Diffusion of univalent ions across the lamellae of swollen phospholipids. *J. Mol. Biol.*, **13**, 238-252 (1965)

Cabane, E.; Malinova, V.; Menon, S.; Palivan, C. G.; Meier, W., Photoresponsive polymersomes as smart, triggerable nanocarriers. *Soft Matter.,* **7**, 9167 (2011)

Erb, E.-M.; Chen, X.; Allen, S.; Roberts, C. J.; Tendler, S. J. B.; Davies, M. C.; Forsen, S., Characterization of the Surfaces Generated by Liposome Binding to the Modified Dextran Matrix of a Surface Plasmon Resonance Sensor Chip. *Anal. Biochem.,* **280,** 29-35 (2000)

Guo, Z.; R€uegger, H.; Kissner, R.; Ishikawa, T.; Willeke, M.; Walde, P., Vesicles as Soft Templates for the Enzymatic Polymerization of Aniline. *Langumuir*, **25(19)**, 11390–11405 (2009)

Hayashi, K.; Shimanouchi, T.; Kato, K.; Miyazaki, T.; Nakamura, A; Umakoshi, H., Span 80 vesicles have a more fluid, flexible and "wet" surface than phospholipid liposomes. *Colloid. Surface B.*, **87**, 28-35 (2011)

Hitz, T.; Iten, R.; Gardiner, J.; Namoto, K.; Walde, P.; Seebach, D., Interaction of α-and β-Oligoarginine-Acids and Amides with Anionic Lipid Vesicles: A Mechanistic and Thermodynamic Study. *Biocheistry*, **45**, 5817-5829 (2006)

Kaneda, Y., Virosomes: evolution of the liposome as a targeted drug delivery system. *Advanced Drug Delivery Reviews.,* **43,** 197-205 (2000)

Käs, J.; Sackmann, E., Shape transitions and shape stability of giant phospholipid vesicles in pure water induced by area-to-volume changes. *Biophys J*., **60**, 825 (1991)

Kuboi, R.; Shimanouchi, T.; Yoshimoto, M.; Umakoshi, H., Detection of Protein Conformation under Stress Conditions Using Liposomes As Sensor Materials. *Sensors and Materials*, **16**, 241-254 (2004)

MacDonald, R. C.; MacDonald, R. I.; Menco, B. Ph. M.; Takeshita, K.; Subbarao, N. K.; Hu, L., Small-volume extrusion apparatus for preparation of large, unilamellar vesicles. *Biochim. Biophys. Acta.,* **1061**, 297-303 (1991)

Manosroi, A.; Wongtrakul, P.; Manosroi, J.; Sakai, H.; Sugawara, F.; Yuasa, M.; Abe, M., Characterization of vesicles prepared with various non-ionic surfactants mixed with cholesterol. *Colloid. Surface B*., **30** 129-138 (2003)

Olea, D.; Viratelle, O.; Faure, C., Polypyrrole-glucose oxidase biosensor: Effect of enzyme encapsulation in multilamellar vesicles on analytical properties. *Biosens Bioelectron.,* **23,** 788-794 (2008)

Omokawa, Y.; Miyazaki, T.; Walde, P.; Akiyama, K.; Sugahara, T.; Masuda, S.; Inada, A.; Ohnishi, Y.; Saeki, T.; Kato, K., *In vitro* and *in vivo* anti-tumor effects of novel Span 80 vesicles containing immobilized *Eucheuma serra agglutinin*. *Int. J. Pharm.*, **389**, 157-167 (2010)

Phillips, M. C.; ChapMan, D., Monolayer characteristics of saturated 1,2-diacyl phosphatidylcholines (lecithins) and phosphatidylethanolamines at the air-water interface. *Biochim, Biophys. Acta.,* **23,** 301-313 (1968**)**

Sato, T.; Kijima, M.; Shiga, Y.; Yonezawa, Y., Photochemically controlled ion permeability of liposomal membranes containing amphiphilic azobenzene.

*Langmuir*., **7**, 2330-2335 (1991)

Shi, G.; Guo, W.; Stephenson, S. M.; Lee, R. J., Efficient intracellular drug and gene delivery using folate receptor-targeted pH-sensitive liposomes composed of cationic/anionic lipid combinations. *J. Controll. Release.*, **80**, 309-319 (2002)

Shimanouchi, T.; Ishii, H.; Yoshimoto, N.; Umakoshi, H.; Kuboi, R., Calcein permeation across phosphatidylcholine bilayer membrane: Effects of membrane fluidity, liposome size, and immobilization. *Coll. Surf. B*, **73**, 156-160 (2009)

Walde, P.; Umakoshi, H.; Stano P.; Mavelli, F., Emergent properties arising from the assembly of amphiphiles. Artificial vesicle membranes as reaction promoters and regulators. *Chem.Commun.,* **50,** 10177-10197 (2014)

Wang, Z.; Cui, H.; Xi, S.; *IC3ME3rd,* 1587 (2015)

Yun, H.; Choi, Y.-W.; Kim, N. J.; Sohn, D., Physicochemical Properties of Phosphatidylcholine (PC) Monolayers with Different Alkyl Chains, at the Air/Water Interface. *Bull. Korean Chem. Soc.*, **24**, 377 (2003)

# General Conclusion

By studying the effects of vesicular membrane on the polymerization reaction of polyaniline, the author was able to clarify how the membrane undulation affected the chemical process and detection of target proteins. In addition, by examining the interaction with enzyme catalysts (proteins), which are essential for chemical reactions, the author was able to obtain guidelines not only for chemical reactions but also for detection of target proteins. These findings would be available for the development of novel chemical reaction process and general biosensors.

Previous studies have examined the fluidity and charge of lipid membranes, but no studies have quantitatively compared the fluctuations of vesicle membranes. It has been found that the fluctuation of the membrane has a significant effect on protein adsorption and stability.

In chapter 2, it was confirmed that GV induced the soft template effect in polyaniline polymerization as well as 100 nm diameter vesicles. Furthermore, a comparison with lipid planar membranes suggests that the membrane undulation was an essential condition for improving the selectivity of ES. Besides, it was observed that the vesicle fission in negatively charged GVs was accompanied with the polymerization reaction, which was in agreement with the necessity of the membrane undulation. Such a drastic deformation of GVs resulted from the insertion of HRP the vesicle membranes to induce their amplified undulation. These event was advantageous for the production of ES. The presence of negative charge on the vesicle membranes contributed to capture the ES as the intermediate of polyaniline polymerization. The series of the process mentioned above was the *soft template effect*.

The continuous undulation enough to fission / budding made it difficult to keep

the reaction field stably over the reaction process. The disruption of vesicles due to their deformation accompanied with the chemical reaction should be controlled. Therefore, the author examined three possible approaches to confer vesicle membrane collapse resistance due to vesicle membrane fluctuations in Chapter 3. First, the coverage of hydrophilic polymers was tested by using several kinds of polymers. Of these polymers, PVP succeeded in the coverage without the disruption of vesicles. For the reason, to reinforce the resistance to membrane disruption is expected. The second approaches is the polymerization of constituent phospholipids of vesicles (liposomes). The calcein leakage experiments indicated no impact of photopolymerization of phospholipids in liposomal membranes on the membrane structure. Besides, no impact on HRP addition was confirmed. Therefore, this approach was not available for the suppressed effect of membrane undulation. Thus, the remaining approaches is the third one, that is, the lining structure of vesicle membranes as mimicking biomembranes. In the present study, this approach was not studied because of the difficulty. It is noted that the biomembrane has adopted the lining structure including cytoskeleton. From these findings, the construction of the lining structure to the vesicle membranes would be promising approach to reinforce the membrane structure against the strong undulation enough to result in the membrane disruption.

In chapter 4, the interaction between vesicles and proteins was clarified by the effect of vesicle membrane fluctuation on the adsorption mechanism. HRP interacted with the vesicle membranes according to the consecutive process. First, HRP was likely to bind to the vesicle membrane based on the electrostatic interaction between accessible Lys on HRP and negatively charged parts of headgroups, followed by the insertion of HRP into membranes under the weak interaction between headgroups of

lipids. This step was driven in a non-electrostatic manner.

In chapter 5, the functions of vesicles have been actually applied as sensor elements and drug delivery system were discussed based on the results obtained in Chapters 2 to 4. Regardless of both the lipid composition of the membrane and the type of proteins with different molecular weight or charge, it was found that the calcein leakage tends to increase with the increase in occupied area due to the protein addition. This suggests that proteins penetrated in the membrane have a sufficient effect on calcein leakage. The strong penetration of protein into vesicle membrane resulted in the morphological change of vesicles from spherical vesicles to erythrocyte or stomatocyte ones. Such dynamical change of vesicle membranes might contribute to the significant leakage of calcein. Previously it has been claimed that the hydrophobic interaction between protein and lipid membrane triggered the calcein leakage. The strength of hydrophobic protein-vesicle interaction would relate to the penetration of protein. These mechanism was obviously based on the nature of the soft interface. It is noted that these results were the first time in the field regarding the protein-induced calcein leakage behavior using the vesicles composed of Span and Tween which are being studied for DDS in recent years. Thus, it can be useful knowledge for the drug delivery system and developing biosensor using proteins.

# Suggestions for Future Works

In this study, the author has studied the membrane undulation characteristics of vesicles, their application to the reaction field, and considerations as sensor materials for a detection of the pathological proteins. As a result, the mechanism of enhanced adsorption of proteins was clarified. This mechanism was based on the nature of soft interface. In the future, it will be necessary to further improve the detection sensitivity of the target protein (10 times or more) and to improve the selectivity (with respect to serum proteins) using a membrane fluctuation resistant vesicle. The various polymer-coated vesicles and polymer-based capsules obtained are expected to be applied not only to detection of specific proteins but also to bioelectronic devices, reaction field materials, and medical engineering. In particular, vesicles having membrane undulation (fluctuations) are expected to be effective reaction fields even when energy is not supplied from the outside, which would be lead to the development of energy saving processes based on the soft materials including vesicles.

# List of Publications

**[Papers]**

1. <u>Saki Fukuma</u>, Toshinori Shimanouchi, Keita Hayashi, and Yukitaka Kimura, Calcein Leakage Behavior from Vesicles Induced by Protein-Vesicle Interaction: A Study by Surface Pressure-Area Isotherms, *Chemistry Letters*, **46(7)**, 1036-1039 (2017)

2. <u>Saki Fukuma</u>, Toshinori Shimanouchi, Kazuma Yasuhara and Yukitaka Kimura, Analysis of partitioning behavior of horseradish peroxidase to phospholipid and surfactant membranes, *Solvent Extraction Research and Development, Japan*, in press.

**[Proceedings]**

1. Toshinori Shimanouchi, <u>Saki Fukuma</u>, Miki Iwamura, Yukitaka Kimura, and Hiroshi Umakoshi, Growth Behavior of Amyloid Fibrils on Membrane Interfaces of Lipid Membranes, Proceedings of the 2016AIChE Annual Meeting, AIChE

2. <u>Saki Fukuma</u>, Toshinori Shimanouchi, Yukitaka Kimura, and Keita Hayashi, Binding of horse radish peroxidase to vesicular membranes for a control of enzymatic polymerization reaction, Proceedings of the ICSST17

3. Toshinori Shimanouchi, <u>Saki Fukuma</u>, and Yukitaka Kimura, High sensitive detection of amyloid beta using the quartz crystal microbalance method combined with the immobilization of lipid membranes,Proceedings of the ICSST17

4. <u>Saki Fukuma</u>, Toshinori Shimanouchi, and Yukitaka Kimura Effect of membrane fluctuation on protein adsorption to lipid membranes,

Proceedings of the 2018AIChE Annual Meeting, AIChE

5.  Toshinori Shimanouchi, Saki Fukuma, Yukitaka Kimura, Miki Iwamura, and Shintaro Deguchi, Effect of Entanglements in Lipid- and Polymer-Planar Membranes on Nucleation of Amyloidβ and Its Fibril Growth Behavior, Proceedings of the 2018AIChE Annual Meeting, AIChE

6.  Saki Fukuma, Toshinori Shimanouchi, and Yukitaka Kimura,
    Effect of Charge and Fluctuation of Vesicle Membranes on the Oligomerization of Aniline, Proceedings of the 2019AIChE Annual Meeting, AIChE

## [International Conference / Symposium]

1.  Toshinori Shimanouchi, Saki Fukuma, Peter Walde, and Yukitaka Kimura,
    Coupling of polyaniline polymerization on giant vesicles with membrane fluctuation. 2015 The International Chemical Congress of Pacific Basin Societies (Pacifichem 2015), Hawaii, United States, December (2015)

2.  Saki Fukuma, Toshinori Shimanouchi, and Yukitaka Kimura, Template Effect of Vesicular Membranes for Polyaniline Polymerization. The 10th Conference of Aseanian Membrane Society, Nara, Japan, July (2016)

3.  Saki Fukuma, Toshinori Shimanouchi, Yukitaka Kimura, and Keita Hayashi,
    Binding of horse radish peroxidase to vesicular membranes for a control of enzymatic polymerization reaction. 11th International Conference on Separation Science and Technology (ICSST17), Busan, Korea, November (2017)

4.  Saki Fukuma, Toshinori Shimanouchi, and Yukitaka Kimura, Effect of membrane fluctuation on protein adsorption to lipid membranes. 2018AIChE Annual Meeting, Pittsburgh, United States, October (2018)

5. Saki Fukuma, Toshinori Shimanouchi, and Yukitaka Kimura, Effect of Charge and Fluctuation of Vesicle Membranes on the Oligomerization of Aniline. 2019AIChE Annual Meeting, Orlando, United States, November (2019)


**[Review]**

1. 島内寿徳, 福間早紀, 木村幸敬, 「膜の動的特性を利用した分子認識/分子変換」 *膜誌*, **41(5)**, 244-249 (2016).

2. 島内寿徳, 福間早紀, 木村幸敬, 「マイクロキャピラリー型水熱反応分離装置の応用技術」, *分離技術のシーズとライセンス技術の実用化*, 122-129 (2018).

3. 島内寿徳, 福間早紀, 木村幸敬, 「誘電分光法による膜界面の微視的ダイナミクス解析」, *表面と真空*, **62**, 205-210 (2019)

4. 島内寿徳, 藤定禎将, 福間早紀, 木村幸敬,「金属ナノ粒子形成を目指した脂質膜上での化学還元法の開発」, *ケミカルエンジニヤリング*, **64**, 26-31 (2019)


**[Article]**

1. 【受賞紹介記事】福間早紀,「ベシクル膜上におけるポリアニリンの重合反応による膜ダイナミクスの解析」, *膜誌*, **41(1)**, 巻頭紹介記事 (2016)

2. 【受賞紹介記事】福間早紀,「ポリアニリンの酵素的重合反応に与える影響〜脂質平面膜とベシクル膜の比較」, *膜誌*, **43(1)**, 巻頭紹介記事 (2018)

3. 【Essay of recipient of session poster prize/査読有】Saki Fukuma, 「Binding of horse radish peroxidase to vesicular membranes for a control of enzymatic polymerization reaction」, *分離技術*, **48(2)**, 38, (2018)

4. 【研究内容紹介記事】福間早紀，「未来博士3分間コンペティション2018 受賞者インタビュー 企業賞(マツダ賞) 次世代研究者インタビュー04」，HIRAKU未来を拓く地方協奏プラットフォーム(代表機関:広島大学 共同実施機関:山口大学，徳島大学)， p18-20，2019年3月発行

# Acknowledgements